www.elsevier.com/locate/jobe

DAYLIGHTING 'ENERGY AND COMFORT' PERFORMANCE IN OFFICE BUILDINGS: SENSITIVITY ANALYSIS, METAMODEL AND PARETO FRONT

Louis-Gabriel Maltais, Louis Gosselin

PII: S2352-7102(17)30102-X
DOI: https://doi.org/10.1016/j.jobe.2017.09.012
Reference: JOBE332

To appear in: *Journal of Building Engineering*

Received date: 24 February 2017
Revised date: 23 September 2017
Accepted date: 26 September 2017

Cite this article as: Louis-Gabriel Maltais and Louis Gosselin, DAYLIGHTING 'ENERGY AND COMFORT' PERFORMANCE IN OFFICE BUILDINGS: SENSITIVITY ANALYSIS, METAMODEL AND PARETO FRONT, *Journal of Building Engineering,* https://doi.org/10.1016/j.jobe.2017.09.012

DAYLIGHTING 'ENERGY AND COMFORT' PERFORMANCE IN OFFICE BUILDINGS: SENSITIVITY ANALYSIS, METAMODEL AND PARETO FRONT

Louis-Gabriel Maltais, Louis Gosselin*

Department of Mechanical Engineering, Université Laval, Quebec City, Quebec, Canada

Abstract

Daylighting performance is an integral feature of sustainable building design. In this paper, two performance criteria were defined, namely an annual glaring index (AGI) and an annual energy requirement for lighting (AEL). Based on 1900 daylight simulations of an office building located in Montreal (Canada), a sensitivity analysis was performed to identify the most influential building design variables among a list of 15. Two sensitivity analysis techniques were employed. Window-to-wall ratios and the overhang dimension were among the most influential parameters for both AEL and AGI, whereas building orientation and aspect ratio, as well as visible transmittance, were found to have a relatively weak influence. A Pareto front demonstrating the optimal tradeoffs between AEL and AGI was approximated from the simulation sample. Finally, a metamodel is developed to calculate rapidly the daylight performance indices for a given set of the 15 design variables.

Keywords: daylight; energy consumption; glare; metamodel; sensitivity analysis; building design

Nomenclature

AEL	annual energy for artificial lighting, (klm-h)/m^2
AGI	annual glaring index
b_{Xi}	linear regression coefficient for each design variable
B_k	window still position for each façade, % of 'available' façade height
CV	coefficient of variation, %

* Corresponding Author: Louis.Gosselin@gmc.ulaval.ca; Tel.: +1-418-656-7829; Fax: +1-418-656-5343.

D depth of overhang for south façade, % of window height

H floor-to-ceiling height, m

L_i illuminance for each point in meshing

VT_n visible transmittance at normal incidence

W/L building aspect ratio

WWR_k window-to-wall ratio for each façade, %

x_i physical design parameter value

X_i normalized design parameter value

Y_i model output value

Greek Symbols

β_{Xi} standardized regression coefficient for each design variable

Δt simulation timestep, hr

η_{lum} luminous efficacy, lum/W

θ orientation angle of the building, °

μ mean

σ standard deviation

1. Introduction

Artificial lighting is one of the most important energy expenditure in buildings. In the US, the Energy Information Administration estimated that 2015 404 billion kWh were used for lighting of residential and commercial buildings, representing 15% of the amount of energy consumed by these sectors [1]. In Canada, according to Natural Resources Canada, lighting generated up to 11% of the energy consumption in the commercial and institutional sectors [2]. There is thus a strong call to reduce the energy consumption of lighting systems. This could be achieved in different ways, such as using more efficient lighting technologies [3] or relying on advanced control strategies [4]–[6]. It is recognized that one can take advantage of daylighting to dim or turn down electric lighting when it is not required, thus reducing the electricity consumption [7].

In addition to the energy concerns of building designers, there is an ever-growing desire to provide the occupants with an access to natural light in built environments. Studies have shown that daylighting affect positively the comfort, well-being and health

of occupants [8]. Furthermore, the behavior of occupants actively seeking daylight in spaces offering manual control over lights and blinds can reduce the consumption of primary energy by up to 40% according to Ref. [9].

Because of its important impact on energy consumption and comfort, lighting occupies a central place during the different design phases of a building. In particular, daylighting performance is thought to be strongly affected by the choices made in the initial design phases such as building orientation and volume, or fenestration ratios. Simulation tools are available to determine the detailed lighting performance of a given building design [10], [11]. However, due to the computational time required, only a limited number of simulations are typically performed in a given project and, as a result, the final design might not be "optimal"[12]. Even though "rules of thumb" exist, truly assessing daylight performance can be quite complex [13]. Because of the multifaceted trade-offs to be made during façade building design, different methods continue to be developed to identify the most important variables in different contexts and to design better façades [14]. Considering all of these observations, the main objective of this paper is to develop a better knowledge of which design parameters are the most significant in the design of a building when it comes to natural lighting performance. In addition, it is desired to develop an easy and fast method to estimate the natural lighting performance of any building design.

In this paper, a set of design variables with their respective range of possible values is used to define a parametric building model (Section 2). In Sections 3, 4 and 5, a global sensitivity analysis is performed to identify the most important variables when it comes to determining the two daylighting performance criteria used in this work. Then a metamodel is developed as a third-order polynomial regression that evaluates these criteria directly from the values of the design variables (i.e. without performing a full simulation). The models and results presented in this paper are focused solely on lighting related aspects of buildings, and could easily be used in an integrated design procedure in which several other considerations could be included, such as overall energy consumption, peak demand, thermal comfort, etc.

2. Building model for lighting simulation

2.1 Description of building design

The building studied in this work is inspired from a real office building located in Brossard, Canada. The building has 5 floors of approximately 2,083 m^2 each and is facing north-west. It received a LEED certification and was built in 2010. The main reason for using this specific building as a "starting point" is that it is currently used to perform a multi-objective optimization and the present study is a part of this work. Nevertheless, it is worth to mention that the methodology introduced here can be used for other buildings and the conclusions presented can be generalized to buildings with similar features.

A series of simplifying assumptions were made when defining the building design in the model. Only one floor was considered in the model. Weather data file for Montréal (Canada) was used for the simulations since it was more easily accessible than that of Brossard. An open plan layout (i.e., the whole floor is considered as an open space area) was considered with a central core of 15 m × 3 m for building services, see Fig. 1. The core was not included in the daylight simulations and its dimensions were kept constant in this study. The reflectivity of the interior surfaces was assumed constant, as well as the floor-to-ceiling height and floor area. For simplicity, the windows were assumed to form a continuous window panel on each façade. An occupancy schedule from 7:30 am to 5:30 pm was assumed, similarly to ASHRAE-90.1's recommendations for building performance simulations. It is important to remember that other schedules would potentially yield different results. The constant parameters of this study are shown in Table 1.

Table 1. List of constant parameters in this study.

Parameter	**Constant value**
Floor area	2083 m^2
Floor-to-ceiling height (H)	4 m
Interior wall reflectivity	0.6
Floor reflectivity	0.2
Ceiling reflectivity	0.8

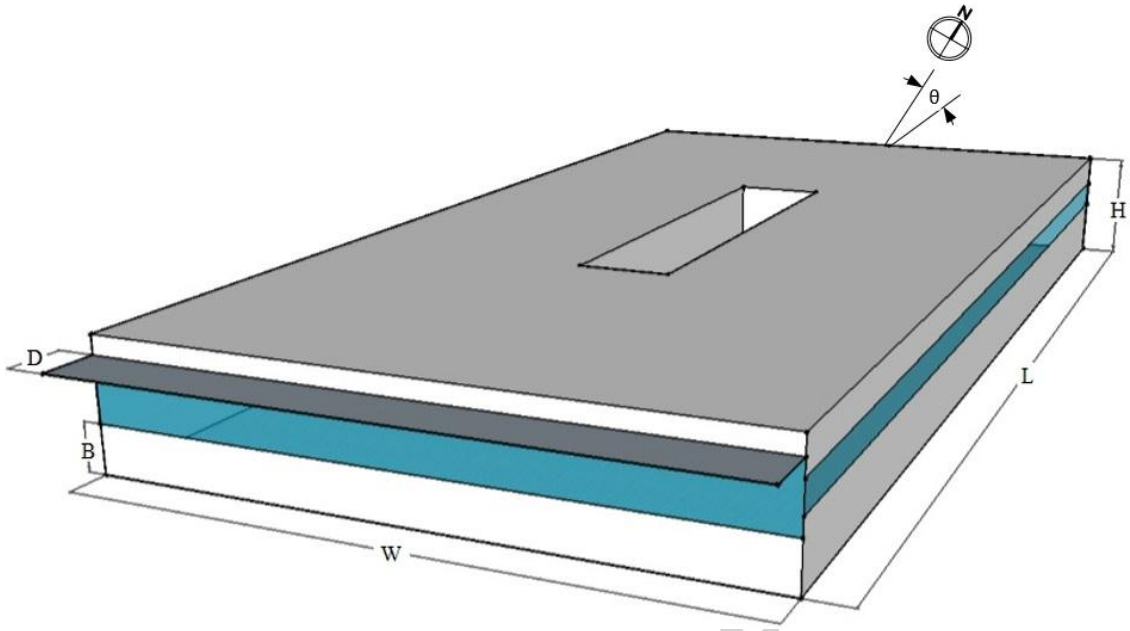

Figure 1. Schematic representation of the building design.

The building design variables that were considered are listed in Table 2, with their respective range of possible values. The building design is characterized by its aspect ratio (W/L), keeping in mind again that the floor area (i.e., WL) is constant, and by the orientation of the building with respect to north (θ). The percentage of the façade occupied by fenestration (window-to-wall ratio, WWR) can be changed independently for each façade, as well as the position of the windows, B, with respect to the floor. The possibility of using an overhang of depth D was also added in the model, but only on the south façade. Finally, the type of fenestration can be changed for each façade by varying the visible transmittance at normal incidence, VT [15]. The range of values for this variable is based on transmittance for windows commonly used in Canada. In the end, the building model is thus characterized by a set of 15 continuous design variables.

Table 2. List of design variables and their respective range of possible values.

Design variables	**Range of possible values**
Building aspect ratio (W/L)	0.2 to 5

Building orientation (θ)	–45° to 45°
Depth of overhang for south façade (D)	0 to 100% of window height
Window-to-wall ratio for each façade (WWR_k)	0 to 70%
Window sill position for each façade (B_k)	0 to 100% of 'available' façade height
Window visible transmittance at normal incidence for each façade (VT_k)	0.426 to 0.762

*Variables with subscript k are assigned per façade (i.e., k = west, south, north, east)

It can be observed that given the range of building orientations in Table 2, any building can be represented by the approach developed in this article since the aspect ratio varies from 0.2 to its opposite fraction (i.e., 1/0.2 = 5). This method was used to avoid any redundancies in the simulations considering that, for example, a building with a 90° orientation is not differentiated from one with a –90° orientation. Orientation is given from north, positive being counter clockwise.

2.2 Daylight simulations

Natural lighting simulations were performed with the software Daysim [16]. The workplane was positioned at 0.8 m above the floor and was meshed with 1000 cells as will be justified in section 2.4.

Different metrics have been proposed over the years to assess daylight performance in the built environment [17]–[19], and this in itself is an active research topic. Here, based on the hour-by-hour daylighting simulation results, two yearly performance indices were developed in order to characterize a building design with a small number of performance criteria. The first criterion is an annual glaring index, AGI.

At each hour of occupation during the simulation, the percentage of the workplane surface area A with an illuminance higher than 2000 lx was calculated. The threshold value of 2000 lx was chosen based on Ref. [20] and a value above that was thus judged to cause glaring. Then, these percentages were summed for all the time steps of the simulation during which the building is occupied, and normalized by the duration of occupation:

$$\mathrm{AGI} = \frac{\sum_{\text{occupied hours}} \frac{A_{\text{above 2000lx}}}{A}}{\left(\text{number of occupied hours}\right)} \tag{1}$$

As a result, AGI is always between 0 and 1. An AGI of 0 means that there is no glaring over the year during occupation hours, whereas an AGI of 1 would mean that the entire workplane surface is always above the recommended threshold.

The second performance index that was considered is a measure of the annual energy for (artificial) lighting, AEL. At each time step during occupation of the building, the difference between the required illumance (500 lx) and the illumance L_i provided by natural lighting is calculated in each cell i of surface area A_i, and then integrated over the workplane, providing a certain number of missing lumens. In other words, it is assumed that these missing lumens (i.e., daylight deficit) are provided by a dimmable lighting system for every cell of the meshing grid (see Section 2.4). Then, by multiplying this number of lumens by the time step, by summing over all occupied time steps and normalizing by the workplane area, it is possible to establish a measure of the energy consumption that would minimally be required by the artificial lighting system per floor area to reach the needed illuminance:

$$\mathrm{AEL} = \sum_{\text{occupied hours}} \sum_{i} \frac{A_i}{A} \mathrm{MAX}\left(500\mathrm{lx} - L_i; 0\right) \frac{\Delta t}{1000} \tag{2}$$

A higher value of AEL means that more energy will be needed for electrical lighting, and vice versa. If needed, AEL could be divided by the luminous efficacy η_{lum} to provide a rough estimate of the energy consumption per unit area (i.e. in kW-h/m^2) for lighting in a high performance building in which lights are dimmed according to the available daylighting. Typically, the U.S. Department of Energy estimated that electrical LED lighting systems have a luminous efficacy η_{lum} between 100 and 150 lm/W [21]. Note

that a similar procedure to evaluate the energy savings was also used in other publications and simulation tools [22], [23]. This approach has the advantage of being general and of not relying on building energy simulations. It does not simulate explicitly the dimming system as it relies solely on daylighting simulations. In other words, it assumes an ideal dimmer that can achieve the "perfect" luminance of each cell of the work plan.

It should be noted that AEL is solely an indicator of the electricity consumption for artificial lighting and does not directly provide the total reduction of the building energy consumption. Interactions of the lighting system with the HVAC system must be considered in order to calculate the actual total energy savings provided by daylighting and dimming strategies (e.g., reducing the recourse to artificial lighting can reduce the internal heat gain which can be beneficial or detrimental to the energy consumption of the building depending on the building considered).

Although not "perfect", these two performance indices (i.e., AEL and AGI) have the merit to characterize quantitatively, and yet simply, the important features of the daylighting performance for a given building design, namely comfort and energy consumption. From a multi-objective design optimization perspective [24], they offer valuable information to accept or reject a design in terms of daylighting performance.

2.3 Impact of workplane mesh

For two specific building designs, Fig. 2 illustrates the value of the two performance criteria, AGI and AEL, as functions of the number of cells in the mesh of the workplane. The calculation times are also reported (for the first building design only since they are very close to those of the second design). It can be seen that above 1000 cells, results become insensitive to further grid refinement, but much more expensive computationally. Therefore, to obtain trustable results, the number of cells was fixed to 1000 for the rest of this work.

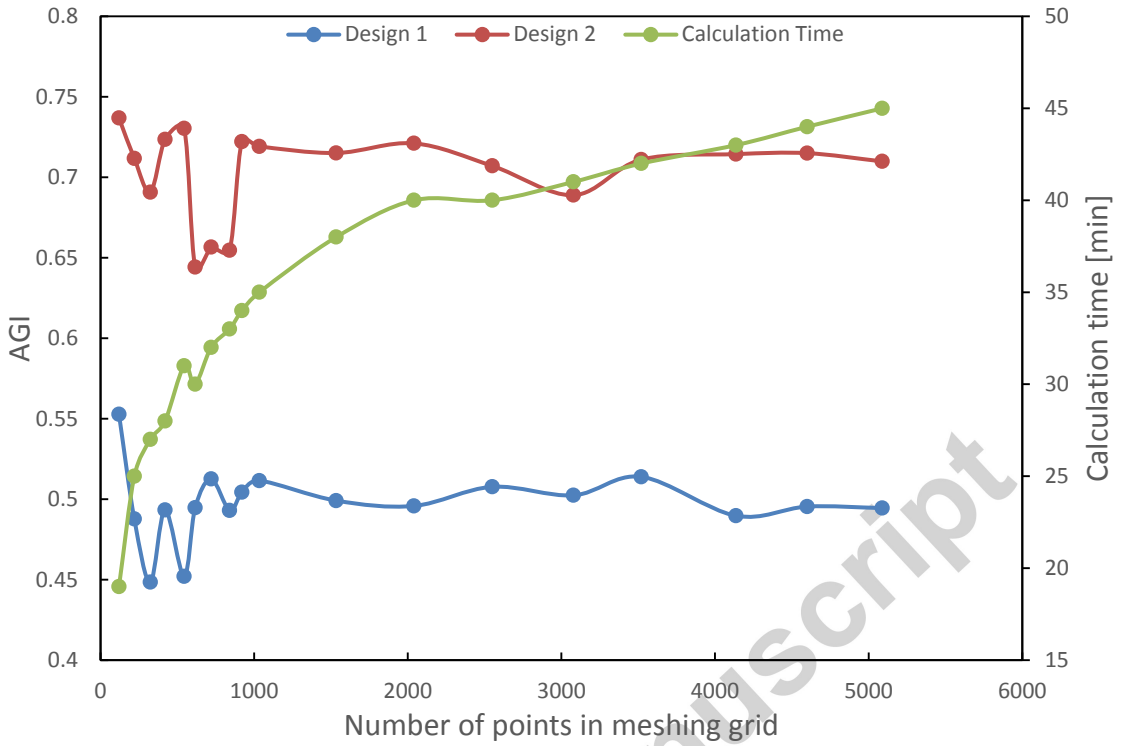

(a)

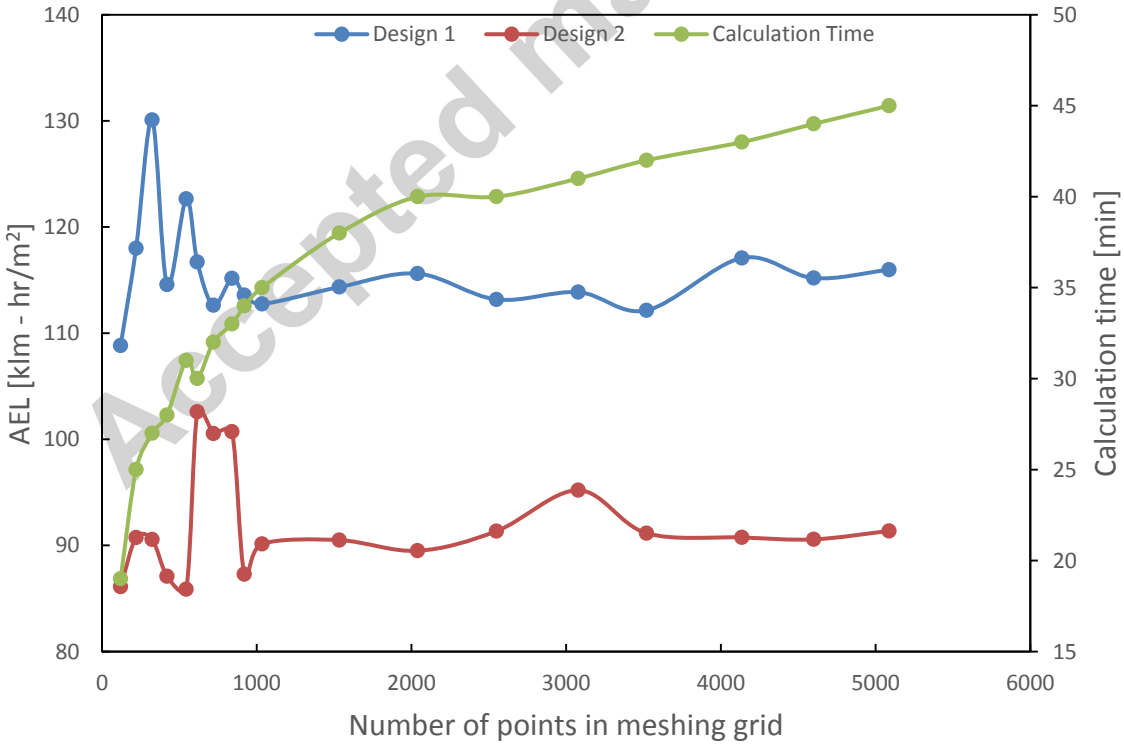

(b)

Figure 2. Mesh independence study for the daylight simulations: (a) AGI and (b) AEL as a function of the number of cells for two cases.

3. Sensitivity analysis

In order to determine the most influential design variables on the two criteria studied in this paper, a sensitivity analysis was performed. A series of building designs was generated randomly based on Table 2. In other words, for each variable, a value of each design variable was randomly taken within its possible range. These random numbers were generated using the "rand" function in Matlab [25]. A relatively large number of possible building designs were generated in this way. Then, each design was simulated as previously described and the daylighting performance criteria were calculated using the results. Using such a "Monte Carlo" sampling methodology, the entire domain could be covered, and as the number of designs increases, the results of the sensitivity analysis stop to change. On the other hand, the size of the sample should be kept as small as possible because of computational time. As seen in Figure 2, a daylight simulation could take around 35 minutes to complete. In other words, for each set of 1000 new designs added to the dataset sample, it requires around 2 weeks of simulation. This emphasizes the importance of selecting a proper sample size.

In a sensitivity analysis, the input parameters must be independent of each other [26]. One could note that even if some of the design variables used in this article might be linked (e.g. the window area, which itself depends on the aspect ratio, is given in terms of wall area percentage), all of these variables can vary independently in their respective range of values and a sensitivity analysis can then be performed.

3.1 Scatterplots

Before the sensitivity analysis, it is interesting to graphically look at the performance indices as functions of the design variables. In fact, the parameters having a strong impact on the outputs can often be found graphically with scatterplots [26]. Indeed, by plotting both outputs as functions of the inputs, it is possible to visually evaluate the impact of a given design parameter. These scatterplots are especially interesting for the most

significant inputs, otherwise they show no clear trends. As an example, Fig. 3 presents graphically the effect of a specific design variable (WWR_S) on AGI and AEL.

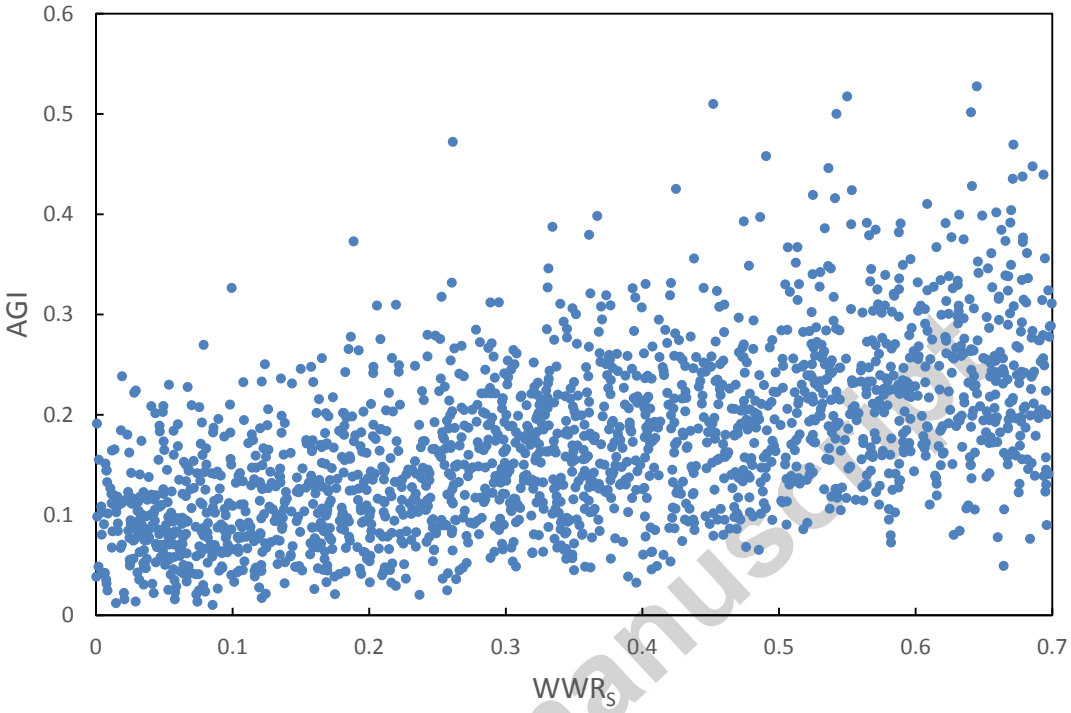

(a)

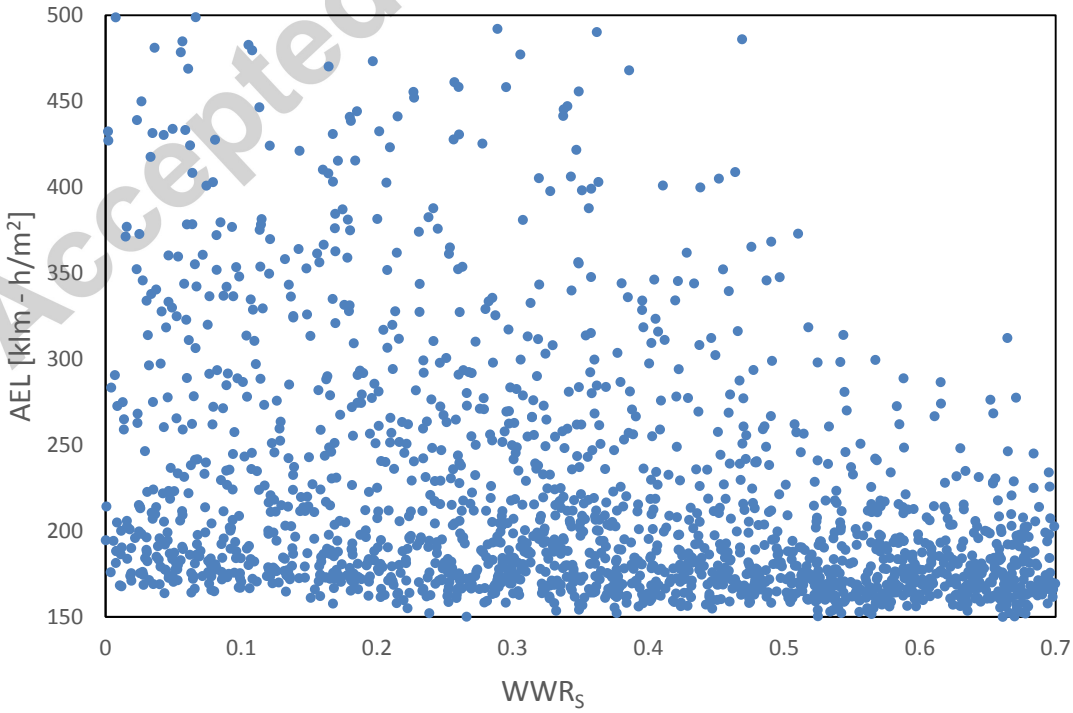

(b)

Figure 3. Scatterplots of (a) AGI and (b) AEL as functions of the window-to-wall ratio of the south façade.

These two scatterplots show an example of a design variable having opposite effects on AGI and AEL (i.e. increasing values of window-to-wall ratio on the south façade increases AGI while decreasing AEL). The fact that design variables often have an opposite influence on the performance indices demonstrates the importance and the difficulty of efficiently choosing their values when designing a building. Also, it can be seen from Fig. 3 that any quantitative conclusion regarding which parameters are important and which are not is difficult using solely scatterplots. This justifies the use of more advanced sensitivity analysis methods as explained below.

3.2 Coefficients of variation

Before the sensitivity analysis is performed, it is worth to verify that the model outputs (i.e. AEL and AGI) actually vary significantly when the design variables are changed. As will be justified below, a series of 500 simulations was first performed. To estimate to what extent the design variables had an impact on the performance indices, the coefficients of variation (CV) for both of them were evaluated:

$$CV_Y = \frac{\sigma_Y}{\mu_Y} \times 100 \tag{3}$$

The symbol Y stands for AGI and AEL. A large CV value means that the corresponding output varies strongly due to changes in the input design variables. The resulting coefficients of variation of AGI and AEL were respectively 49.1 and 56.7% for 500 simulations and their evolution with the number of simulations is shown in Fig. 4. This illustrates that the design variables have a large impact on both criteria and also justifies the use of the indices proposed in this article because they are highly affected by the input values.

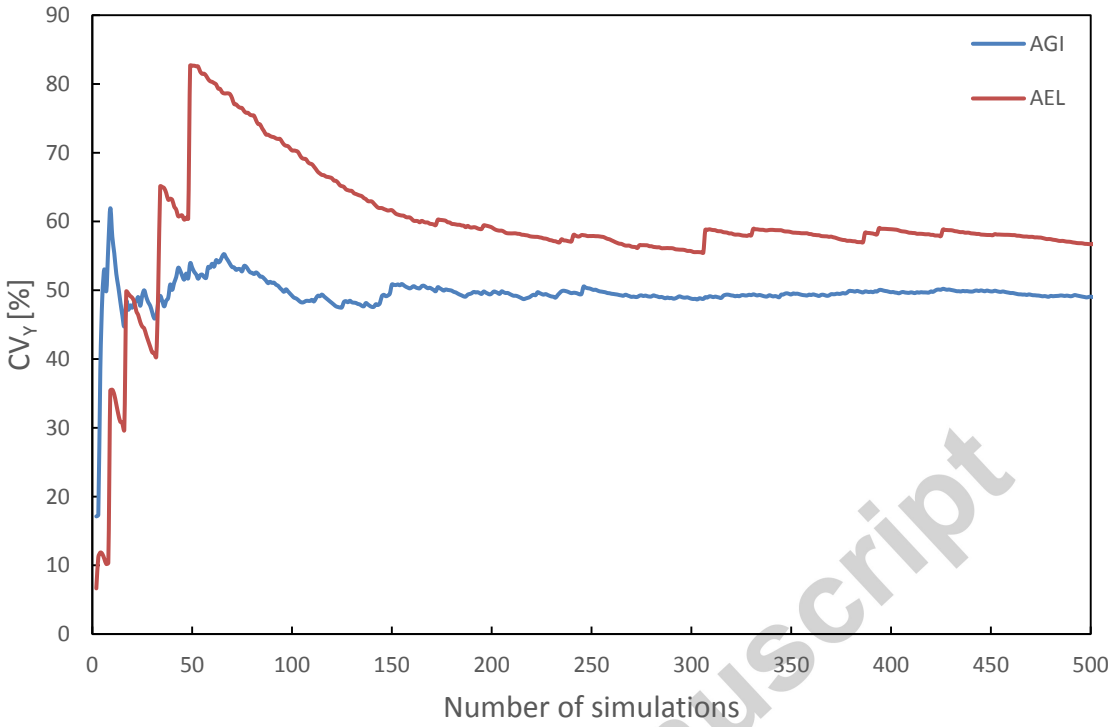

Figure 4. Coefficients of variation for AGI and AEL as functions of the number of simulations.

The CV coefficients are useful when it comes to verifying if the selected design variables have an impact on the outputs, but provide no information about their individual effect. In order to determine the most influential variables, two techniques were employed. First, a linear regression is built and based on the value of the weights, the most influential variables are found (Section 4). Second, a formal variance decomposition technique is applied to the dataset to calculate the first-order and second-order sensitivity coefficients (Section 5).

4. Standardized regression coefficients and linear regression

4.1 Description of the method

Linear regressions can be used conveniently to determine which design variables have the most important impact on the variation of the performance indices. First, the 15 design variables have all been rescaled to range from 0 to 1. This has to be done to account for the differences in the range of possible values for the variables, some having a span of values smaller than 1 (e.g. visual transmittance) while others are as large as 90 (e.g.

orientation). These normalized variables are called X_i, with i ranging from 1 to 15. The relation between the physical design variables (x_i) and the rescaled X_i is simply:

$$X = \frac{x - x_{\min}}{x_{\max} - x_{\min}} \tag{4}$$

The main idea behind the linear regression approach is to estimate values of the model outputs (i.e. AGI and AEL) by using a linear combination of the scaled design variables:

$$Y_n^* = b_0 + \sum_{i=1}^{15} b_{x_i} X_i \tag{5}$$

where Y can be either AGI (i.e. n=1) or AEL (i.e. n=2). The star symbol means that this relation provides an estimate of Y. Two sets of b_i's can be found, one for AGI and one for AEL. The weight coefficients b_i are found by minimizing the quadratic error between the calculated and the estimated values of the indices considering all the simulation results:

$$E = \sum_{j=1}^{numsim} (Y_n - Y_n^*)^2 \tag{6}$$

Then, standardized regression coefficients (SRC) are used to evaluate the sensitivity of a variable X_i on the output Y:

$$\beta_{X_i} = b_{X_i} \frac{\sigma_{X_i}}{\sigma_Y} \tag{7}$$

The SRCs are actually a more robust version of the usual regression coefficients [26]. More specifically, the SRC values represent the change in the standard deviation of an output for a change of one standard deviation in an input, with all others being kept constant [26]. In other words, they provide an insight on the impact of each design parameter on the outputs. A large β_{X_i} value means that the variable X_i has a lot of influence on the model output (i.e. either AGI or AEL), and vice versa, a small β_{X_i} value means that the variable X_i does not influence the model output.

4.2 Required number of simulations

The number of random simulations was increased until the value of the SRCs stopped to evolve. Every 50 simulations, the SRCs were recalculated and compared to the previously calculated ones as illustrated in Fig. 5. The evolution of the coefficients of

variation introduced in the beginning of this section is also shown in this figure. It can be seen that ~600 simulations are sufficient to ensure stable results for the linear regressions.

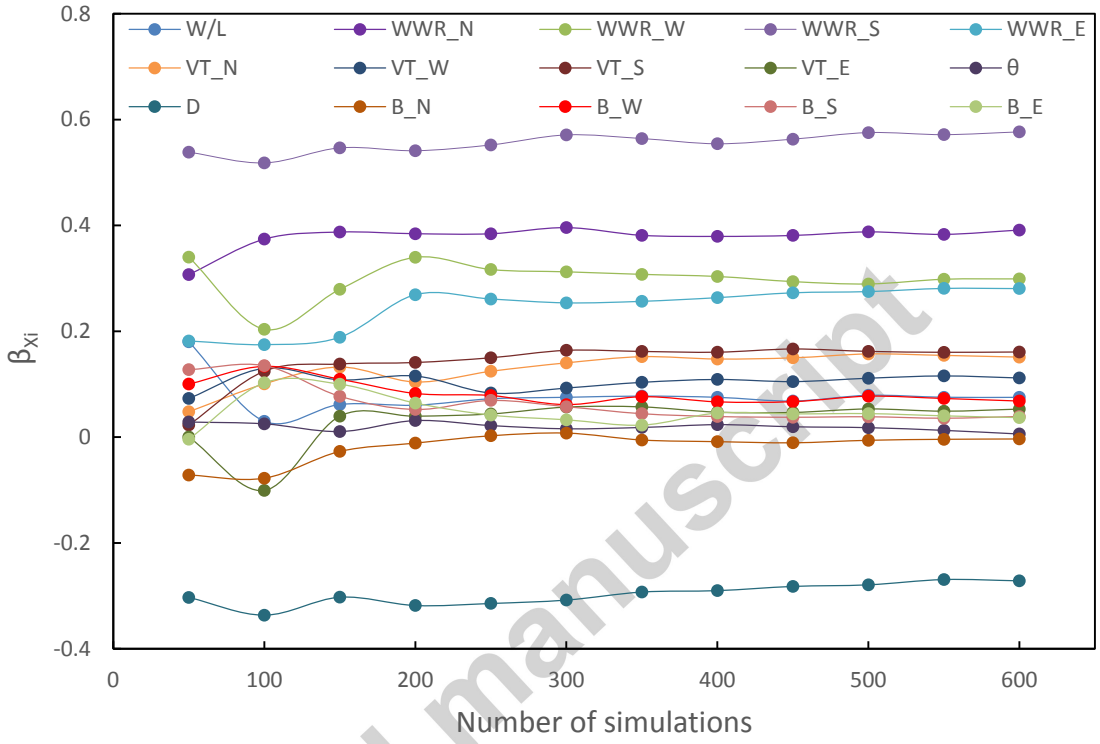

(a)

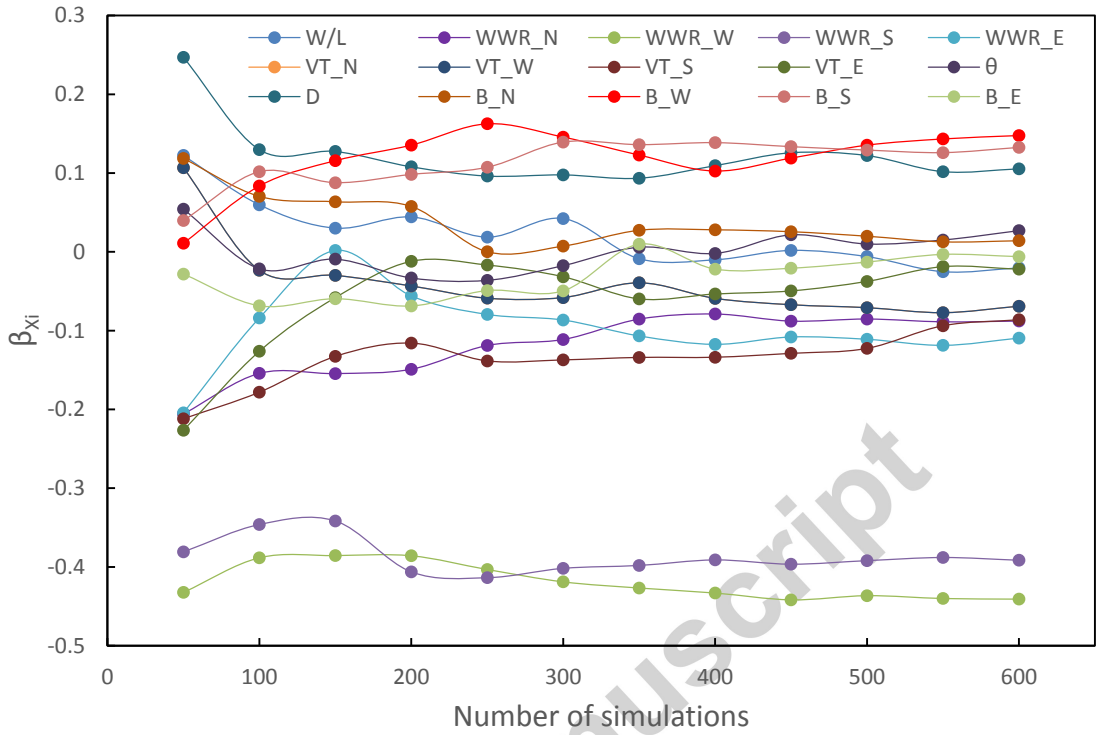

(b)

Figure 5. Standardized regression coefficients as functions of the number of simulations for: (a) AGI and (b) AEL.

4.3 Results: Standardized regression coefficients (SRC)

The 15 resulting coefficients, one for every design variable, are shown in Fig. 6 for both model outputs, i.e. AGI and AEL. Before analyzing these results, it is worth to evaluate whether the linear models developed in this section can successfully estimate the outputs values by verifying the value of the sum of the squares of the SRCs. A sum close to 1 means that the linear fitting can "perfectly" predict the outputs [26]. In the present case, $\sum \beta_{X_i}^2$ is equal to 0.805 and 0.449 respectively for AGI and AEL. This means that a significant part of the variance of AGI and smaller part of the variance of AEL can be explained by a linear model, the rest being explained by higher orders behaviors. Therefore, the linear regression approach can provide a rough estimate of the influence of each variable, but the presence of non-linearity, especially for AEL, justifies the use of a more advanced technique (as that of Section 5).

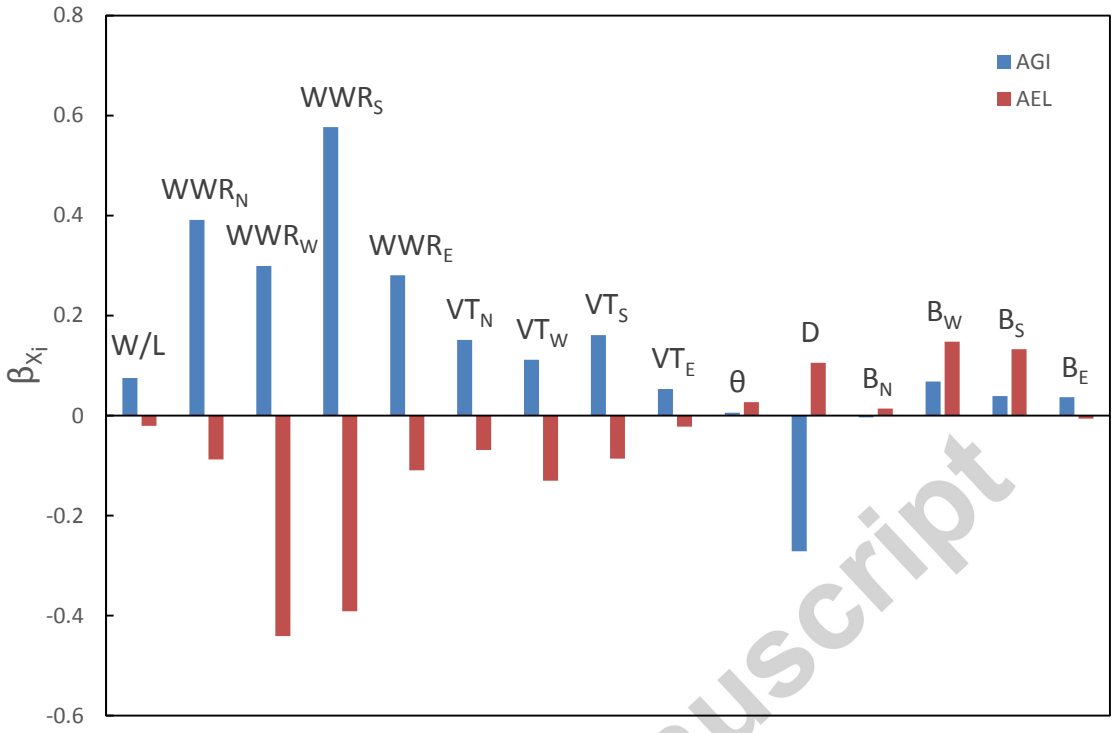

Figure 6. Standardized regression coefficients for every design parameter and both performance indices (AEL and AGI).

First, the performance with respect to glaring, i.e. the criterion AGI (blue in Fig. 6), will be analyzed. It can be seen that the most influential variables are the window-to-wall ratios, and in particular that of the south façade. WWRs were also identified as the most important design variables in terms of energy and visual comfort in Ref. [27] for an office building in hot-dry climate. The standardized regression coefficients are all positive for these variables, which means that increasing the window-to-wall ratios increases glaring. This is expected since the daylight availability ratio increases with this variable for every orientation [5]. The second most influential variable on the glaring is the dimension of the shading system. This regression coefficient being negative, it means that a deeper overhang helps protecting against glaring (i.e., it reduces AGI). The other variables (i.e., building aspect ratio and orientation, window transmittance and position windows) exhibit a smaller impact on glaring according to the linear regression.

The impact of the design variables on the required electric lighting (i.e., on AEL) was also investigated with a linear regression and is reported in Fig. 6 with red lines. The most positively influential variables are the ones related to the vertical position of the

windows, and in particular for the west and south façades. The regression coefficients being positive means that windows located at a higher position on the façade (remembering that the workplane is at a height of 0.8 m) tend to increase the requirement for electrical lighting. The size of the overhang shading system and the window-to-wall ratio for the west and south façades were also found to be relatively influential. Considering the sign of the regression coefficients, one can see that smaller south or west windows and larger overhang increase AEL (i.e., the requirement for artificial lighting). The west and south façades are the ones receiving the most important amount of annual total solar radiation during occupancy, which might explain why they were particularly influential [28]. The impact of the other variables (i.e., building orientation and aspect ratio, WWR of north and east façades, window transmittance) on the artificial lighting requirement is found to be small based on the linear regression.

One can note the relatively small SRC values of all visible transmittances, especially for AEL. This means that the choice of a window (as along as its visible transmittance is in the selected range of possible values) would have only a marginal influence on the required energy consumption for artificial lighting. This might come from the selected range of transmittance which was chosen to represent the Canadian context. Windows in Canada are more commonly chosen in a heating context and an important driver for window selection is the solar heat gain coefficient (SHGC). A wider range of transmittance might have resulted in larger SRC values, but would have been less realistic.

The other parameters that did not prove to be particularly influential based on the linear regression are the shape and orientation of the building. This result might come out as a surprise since current trends in architectural design (e.g., bioclimatic or integrated design) devote significant attention to the elaboration of building volume and shape [29]. This result might be due in part to the fact that both performance criteria come from summation over the entire floor surface area. Keeping the area constant for all simulations might have reduced the impact of the geometry of the buildings. Also, only a box-building shape was simulated, i.e. other shapes such as L or H were not investigated, which again can reduce the overall impact of building orientation and aspect ratio. Higher order effects and interactions with other variables could increase the influence of the

shape and orientation of the building. Finally, it should also be noted that other aspects of building design such as the heating and cooling needs or urban structure could also dictate or influence building shape and orientation in addition to daylighting [30].

5. Variance decomposition

Since the weak linearity of the AEL output is demonstrated by the linear regression ($\Sigma\beta_i^2$=0.449), the use of a more advanced sensitivity analysis technique had to be considered. The interactions between variables are not necessarily negligible since, for example, a variable might have no influence on the outcomes alone, but be influential when paired with another one. To do so, a variance-based method (Sobol sensitivity analysis) as shown in [26] and [31] was applied to the dataset.

5.1 Description of the method

For N inputs variables X, the variance of an output Y can be decomposed as

$$V(Y) = \sum_i V_i + \sum_i \sum_{j>i} V_{ij} + \sum_i \sum_{j>i} \sum_{k>j} V_{ijk} + \ldots + V_{12\ldots N} \quad (8)$$

where V_i is the variance of the expected value of the output Y for every value taken by X_i, as shown below:

$$V_i = V(E(Y \mid X_i)) \quad (9)$$

For the higher-order indices, one has to subtract the effect of the lesser-order effects. As an example, V_{ij} (i.e. second-order sensibility indices) is calculated as

$$V_{ij} = V(E(Y \mid X_i, X_j)) - V_i - V_j \quad (10)$$

Then, the value of the sensibility indices is obtained by dividing both sides of (8) by V(Y):

$$1 = \sum_i S_i + \sum_i \sum_{j>i} S_{ij} + \sum_i \sum_{j>i} \sum_{k>j} S_{ijk} + \ldots + S_{12\ldots N} \quad (11)$$

The first-order sensitivity indices (S_i) represent the contribution of an input to the variance of an output variable. In other words, a large S_i value means that the variable X_i influences the model outputs whereas a small S_i indicates that the variable X_i does not influence the model outputs. Just as the SRCs introduced earlier, the S_i-values show the impact of each individual parameter on the performance indices. Thus, they are equal to

the square of the SRCs when the model is linear. Higher order sensitivity indices take into account the interactions between the different design variables.

These sensitivity indices were determined with the EASI algorithm. This method is a Fourier-based technique that, by using a frequency-based approach to perform variance-based sensitivity analysis, has the ability to evaluate first-order and higher order indices [32].

5.2 Required number of simulations

The number of simulations had to be increased for the calculation of the Sobol indices since, for small sample sizes, the values of the first-order indices tend to be over-estimated by the algorithm [32]. This typically results in a summation of the first-order indices larger than 1 which is not in accordance with the variance decomposition of Eq. (11). Keeping in mind the computational cost of adding more simulation results to the dataset of samples, the number of simulation results was gradually increased. The sum of the first-order Sobol indices is shown in Fig. 7 as a function of the number of simulations. It can be seen that the over-estimating bias is significantly reduced with ~1900 simulations, which is the number of simulations used for this section.

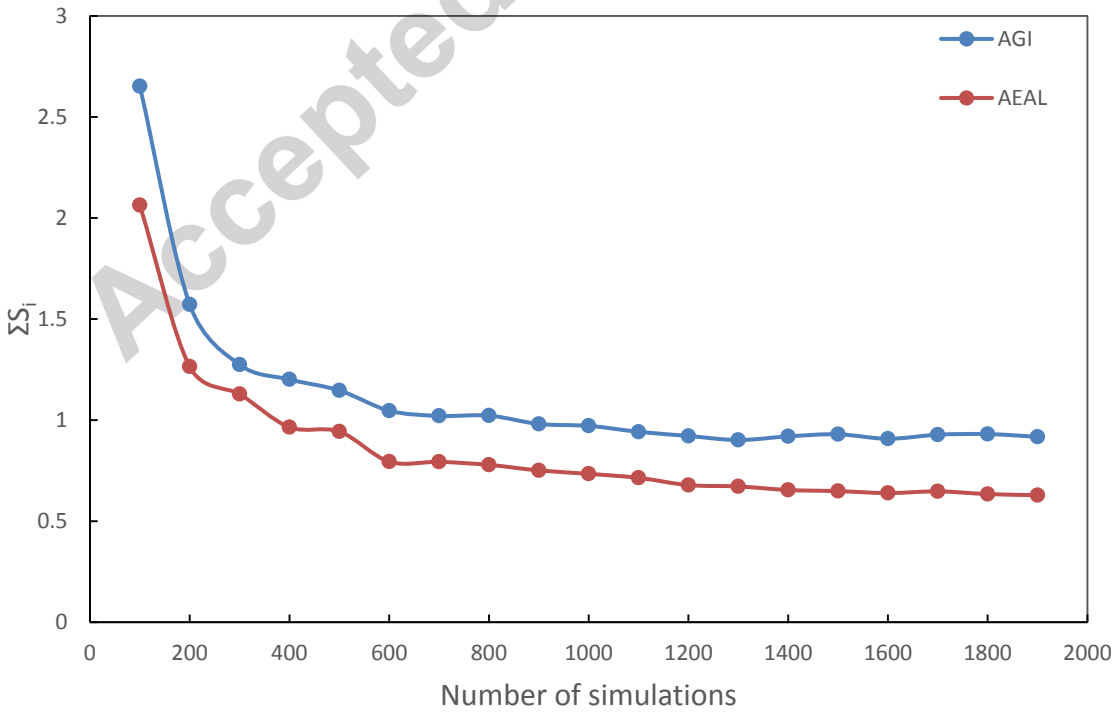

Figure 7. Summation of the first-order sensitivity indices as a function of the number of simulations.

5.3 Results: First-order effects

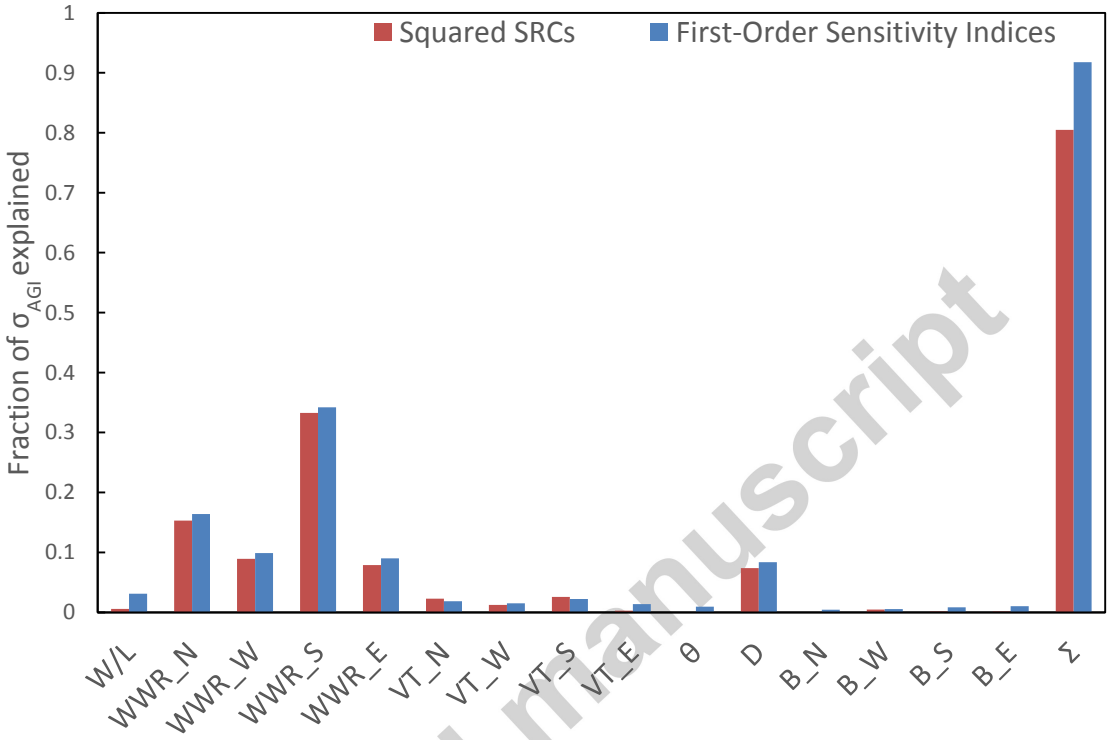

(a)

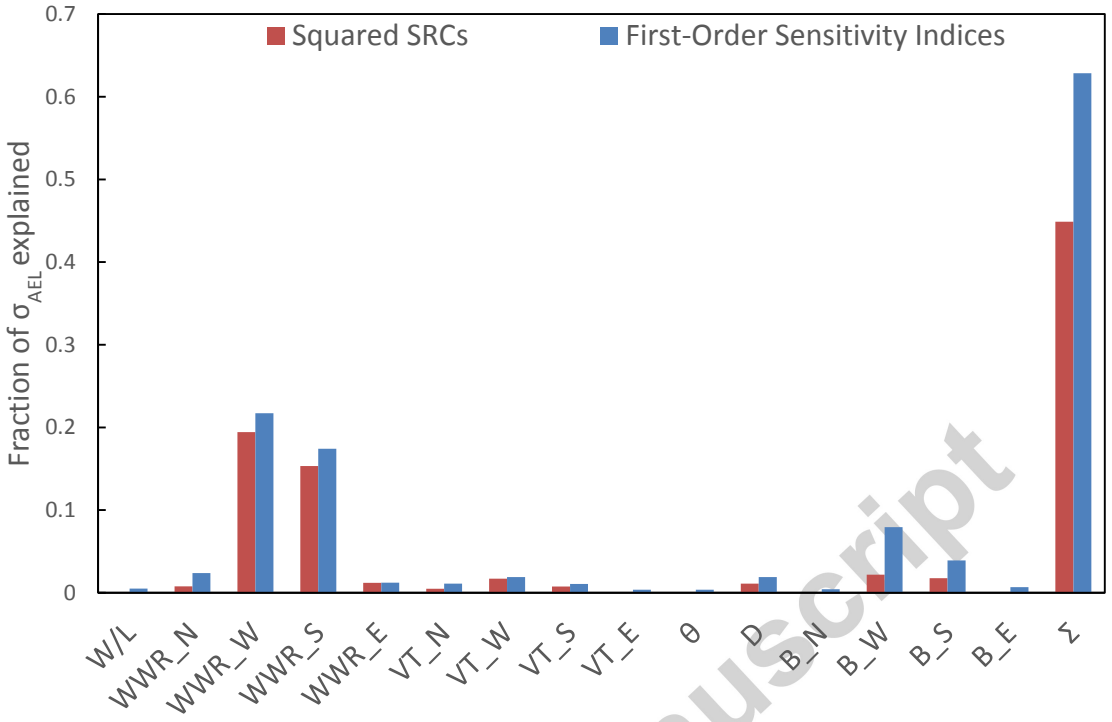

(b)

Figure 8. First-order sensitivity indices and square of standardized regression coefficients as functions of the design variables for: (a) AGI and (b) AEL.

Figures 8a and 8b report the first-order indices for AGI and AEL respectively, along with the square of the SRC values. As expected, the first-order indices are very close to the squared SRCs values for AGI, since the linearity of the model was relatively good in that case. On the other hand, the SRC values for AEL are relatively different from the first-order indices. This is explained by the fact that this performance index does not have a strong linear behavior, as previously mentioned. It is important to note that, even with different values, both the SRCs and the first-order indices tend to result in the same ranking of the most influential variables. Since the most influential variables have already been analyzed in Section 4, this discussion will not be repeated here. It is also interesting to note that the sum of the first-order indices reaches 0.628 and 0.917 for AEL and AGI respectively, which is also a measure of the linearity in the model [26].

5.4 Results: Second-order effects

The interactions between two variables can be evaluated by calculating second-order indices (i.e., the S_{ij} terms in Eq. (11)). The results are shown in Figures 9a and 9b for AGI and AEL respectively.

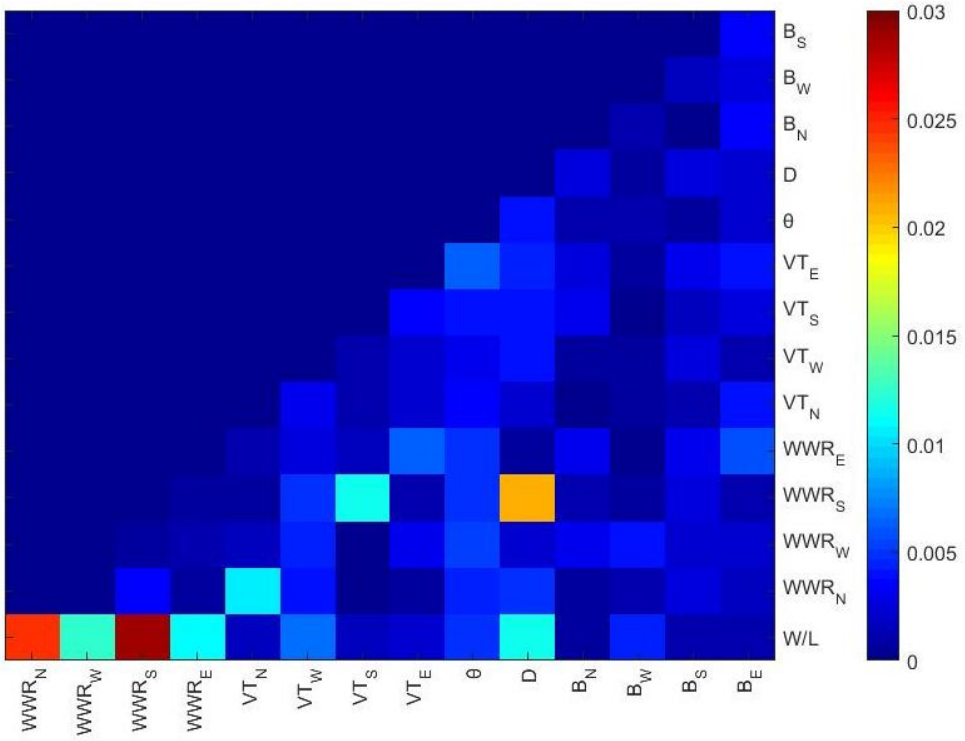

(a)

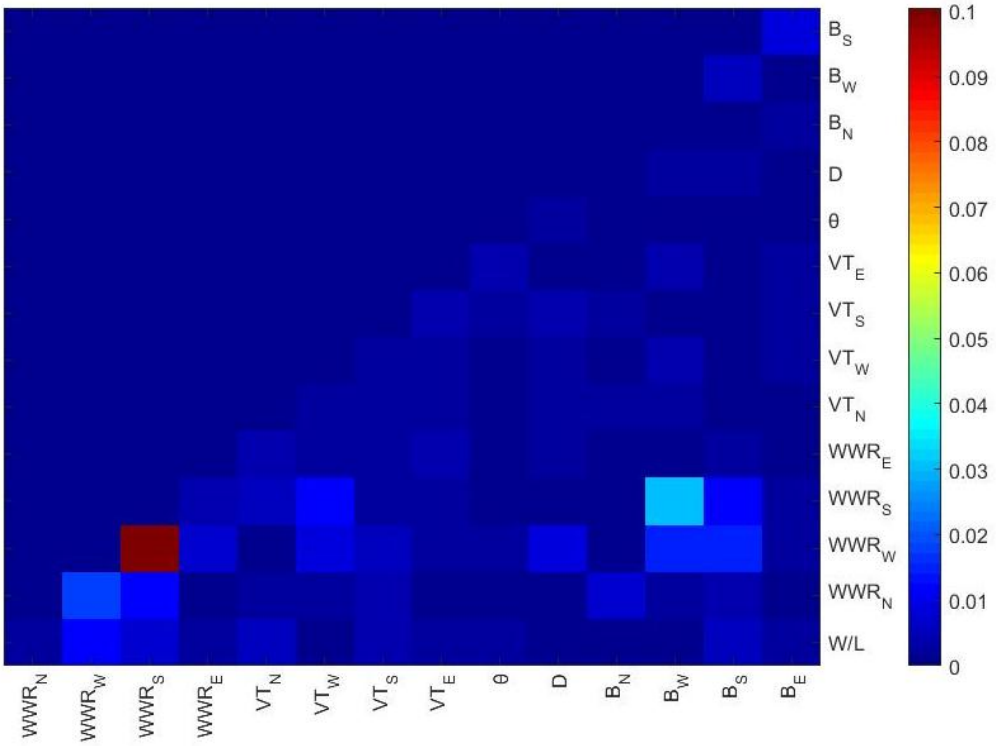

(b)

Figure 9. Second-order sensitivity indices as functions of combination of design variables for: (a) AGI and (b) AEL.

First, the interactions for the glaring index are analyzed. As expected, the second-order indices for AGI are smaller than the first-order indices (because of the relative linearity of the model), with respective summations of 0.349 and 0.912 respectively. This means that the sum of both orders of indices reaches 1.261. A summation higher than 1, i.e. an over-estimation of the indices, is an indication that the sample size might have to be increased to achieve a more precise variance decomposition. However, given the objective of this paper, which is to identify the most influential design variables and interactions and not to achieve a precise variance decomposition, results were considered acceptable. Furthermore, the overestimation is relatively small.

The second-order indices for AGI (Fig. 9a) demonstrate the importance of the interactions between the building aspect ratio (i.e., W/L) and the window-to-wall ratios of all façades (i.e., WWR). This is explained by the fact that the glare depends on the surface area of the windows, which is proportional to the product of the building width or length and the window-to-wall ratios. Also, the depth of overhang (i.e., D) and the visual

transmittance of the south façade (i.e., VT_S) are linked to the window-to-wall ratio for that façade. This highlights the interest of considering these parameters together when designing a building.

The sum of the first and second-order indices for AEL is also slightly higher than 1 with a value of 1.07 (i.e., sums of 0.439 and 0.628 for the first and second-order respectively). For the same reasons as above, the results were considered acceptable. Important interactions were expected because of the non-linearity of this performance index. The second-order index between the window-to-wall ratios of the south and west façades has the largest value, i.e. 0.100. This is likely due to the fact that these orientations are the most exposed to sun irradiation. In addition, daylight entering from the west window and being reflected on the inner surface of the south window (and vice versa) can affect the performance indices, thus increasing the importance of the interactions between these parameters. Other interactions between parameters such as WWR_S and the windowsill position for the west façade (i.e. B_W) or WWR_W and B_W show the importance of reflections of light on internal surfaces to achieve the required illuminance level and thus, the relevance of choosing simultaneously appropriate values for these design parameters.

6. Pareto front

6.1 Minimal AEL versus minimal AGI

From a design perspective, one would be interested to minimize simultaneously both AEL (i.e., reduce at most the use of artificial lighting) and AGI (i.e., visual discomfort due to glare) [33]. Results presented in the preceding sections have shown that the design variables often affect these objectives in opposite directions. In other words, reducing AGI can increase AEL and vice versa. Fig. 10 reports the values of AGI and AEL for all the simulations that were performed in the course of the present paper. Each point in that figure corresponds to the result of a simulation. Fig. 10 can be seen as an illustration of the accessible design space based on the sample of simulations. It also reveals the shape of the Pareto front which contains non-dominated designs (i.e. for a given AGI value, the minimal AEL value that could be achieved and vice versa). The approximate position of the Pareto front is shown with a dashed line. All designs on that line (i.e. the red dots) can

be considered the best in the dataset from a multi-objective point of view. The selection of a specific design along the front depends on the weight given by the designer to each of the two objectives individually (AEL vs AGI). It should be noted that the dashed line is the *estimated* Pareto front shape based on the dataset: since no formal multi-objective optimization was performed, the exact position of the front might be slightly different.

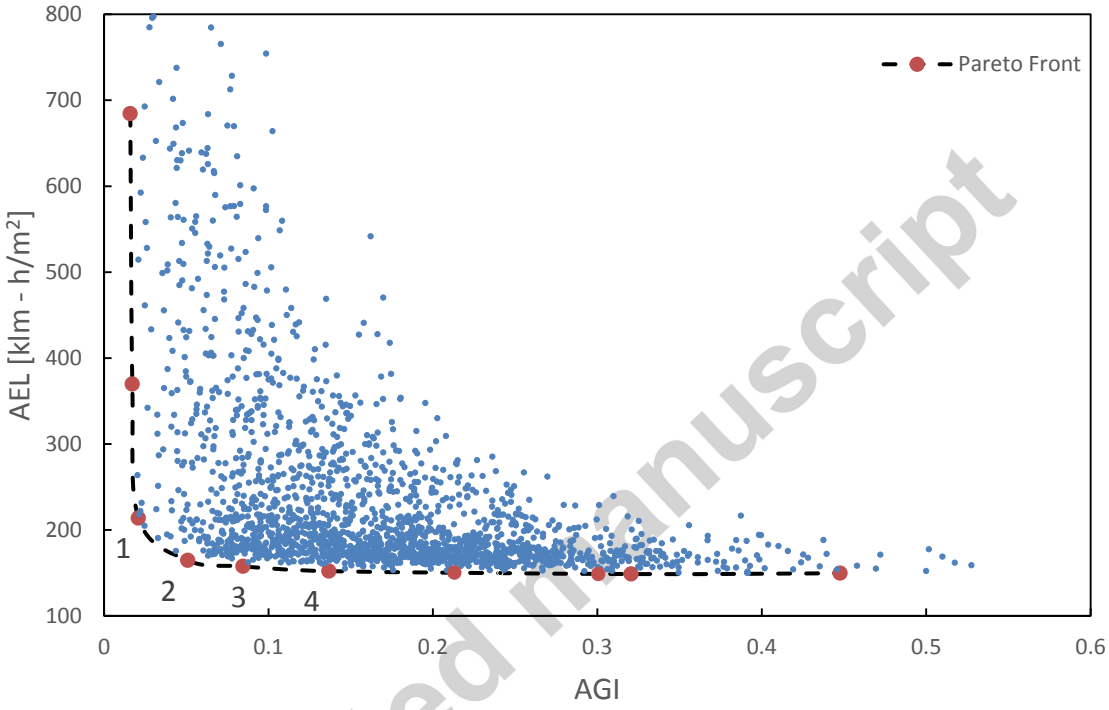

Figure 10. AEL versus AGI for the simulations performed in this paper and illustration of the Pareto front.

Fig. 10 shows that many designs can provide a low value of AEL (AEL ~ 150 klm-h/m^2) but often with a large AGI value and similarly, several designs exhibit low AGI values (AGI ~ 0.02) but often with high AEL values. On the Pareto front, AEL varies from 148 to 685 klm-h/m^{2}and AGI, from 0.016 to 0.448. For the sake of illustration, with a luminous efficacy of 100 lm/W, the AEL values correspond to approximate lighting energy between 1.5 and 6.85 kWh/m^2 [34].

It is also interesting to note that small values of AEL are observed for a lot of the designs. In other words, the density of points in Fig. 10 is high for low AEL values. However, the density of points at low AGI is low. This means that achieving good

designs in terms of glare avoidance might prove more difficult than identifying low lighting energy designs.

6.2 Weight of the indices in terms of building performance

Before presenting the detailed features of the designs on the Pareto front, it is worth discussing about the weight or importance of each of the performance index in a design. Choosing the right design on the Pareto front is a matter of whether more importance is put on AGI or AEL by the designer through a multi-criteria decision analysis. In this section, an economic comparison is attempted.

First, the impact of AGI can be converted into costs by linking it to a decrease in productivity due to glaring. More specifically, by multiplying the AGI by the number of employees, their salary and a given decrease in productivity, it is possible to estimate the economic loss associated to a given AGI value. As an example, for 70 employees and 50% of them performing tasks that are influenced by lighting, an annual salary of 50 000$ and a decrease of 10% in productivity due to improper lighting [35], the following relation can be found:

$$Loss[\$] \sim 175,000 \times AGI \tag{12}$$

Using the mean value of the AGI calculated over the entire sample used in this work (which is of 17%), economic loss, i.e. maximum potential savings related to optimizing AGI, reaches ~29 000$/year. However, it should be noted that blinds could be used to reduce glare, and that the influence of glare is task-dependent. Therefore, that value should only be taken as an order of magnitude of the potential economic impact of glare.

Similarly, AEL can be related to an energy cost. In fact, several studies have demonstrated a direct relation between daylighting optimization and energy savings. For example, Ref. [36] achieved a reduction of 30% in energy consumption by optimizing daylighting use. As mentioned previously though, caution should be exercised in analysing energy savings based on AEL since this value is solely an indicator of the energy consumed by the artificial lighting system and does not account for the potential interactions with the HVAC system. Nevertheless, it is possible to estimate the potential savings in terms of artificial lighting. By performing an analysis similar to the one above, the maximum potential lighting energy savings can be estimated for the worst-case

scenario where there is no daylighting. Using a value of 21 kWh/m^2 in the office space to provide artificial lighting for the occupied hours (2080 hours), and multiplying by the floor area (2083 m^2) and the cost of electricity (approximately 0.1 CAD/kWh), these savings are evaluated to 4,400$. More generally, AEL (in klm-hr/m^2) can be linked to an estimation of the potential savings with the following equation, where the luminous efficacy is approximated to 100 klm/kW (as discussed in Section2.2):

$$Savings[\$] = \frac{AEL}{\eta_{lum}} \times Area \times \frac{0.1 CAD}{kWh} = 2.08 \times AEL \quad (13)$$

Again this saving is just for the energy consumption of the lighting system and does not account for interactions with the HVAC system. As an example, for the worst AEL of the sample produced in this work (i.e., 1,507.91 klm-hr/m^2), the savings can reach ~3141$, which is, as expected, under the maximum potential savings since it takes into account daylighting.

The numbers mentioned above illustrate that the cost of AGI can be more important than that of AEL. However, the estimation of the AGI cost is somewhat uncertain and arbitrary, whereas that of the AEL is related to "concrete" monthly energy bills. All in all, this demonstrates that both criteria are relevant and impactful, and should be considered simultaneously. These considerations should be kept in mind while choosing the best trade-off in terms of building design, as discussed in the next sub-section.

6.3 Recommendations and guidelines for building design

As mentioned above, the Pareto front gathers the optimal designs from the simultaneous consideration of both AEL and AGI. Therefore, by analyzing the features of the designs on this front (i.e. optimal designs), it is possible to establish guidelines regarding the choice of design variables to achieve an optimal daylight performance. In the end, the selection of a design on the front among the different possibilities is up to the designer and depends on the importance given to one criterion with respect to the other (see Section 6.2).

Some of the building designs on the Pareto front (see numbered red dots in Fig. 10) are reported in Table 4. As one moves in the direction from point #1 to point #4 on

the Pareto front, the overall percentage of fenestration increases: this corresponds to moving from high AEL/low AGI designs to low AEL/high AGI designs. In this direction, the overall WWR of the building designs is 9%, 13%, 21% and 27% for points 1 to 4, respectively. The WWR for the west façade tends to be high for all four points, whereas that of the other façades increases from very low values at point #1 to higher values at point #4. In [37], it was found that WWRs above 30% only yielded small improvements in terms of energy saving from daylighting which is in line with the designs observed on the present Pareto front. Again, these common features of the designs on the Pareto could be used as guidelines for building designs with optimal daylight performance.

The overhang dimension, which was also one of the most influential parameters, do not exhibit a clear trend for points #1 to #4 since the WWR of the south façade (where it is installed) is very small and, as a result, the overhang does not play a significant role for these four designs. The west window vertical position on the façade was another influential variable (for AEL in particular). The trend for points 1 to 4 is to have the windowsill relatively close to the floor.

In addition, the visible transmittances tend to be in the upper range of the possible range. Even if their influence was found to be small in the sensitivity analysis, the best designs forming the Pareto front exhibit high visible transmittance. It is important to note that these design recommendations are made from a daylighting perspective only and that no thermal analyses were performed. The guidelines developed in this section could be used in parallel with a thermal analysis.

To summarize, the common features of the optimal designs for the current case are: low WWR for east, north and south façades, window sill close to the floor on the west façade, high transmittance.

Table 4. Design parameters values for non-dominated points forming the Pareto front.

Points	W/L	WWR_N	WWR_W	WWR_S	WWR_E	VT_N	VT_W	VT_S	VT_E	θ	D	B_N	B_W	B_S	B_E
1	4.204	0.013	0.498	0.073	0.082	0.731	0.434	0.656	0.440	-29.028	0.252	0.249	0.222	0.003	0.260
2	2.964	0.066	0.424	0.133	0.022	0.465	0.756	0.602	0.709	-19.235	0.424	0.926	0.028	0.479	0.736
3	3.547	0.169	0.657	0.168	0.090	0.647	0.738	0.723	0.570	41.697	0.834	0.122	0.147	0.192	0.631
4	0.832	0.318	0.315	0.239	0.224	0.605	0.693	0.675	0.611	20.929	0.266	0.893	0.175	0.197	0.146

In order to include AEL and AGI in a global multi-objective problem that would consider these criteria among others, it is worth to develop a metamodel that could calculate these indices quickly, which is the purpose of the next section. Furthermore, such metamodel could help to precise the shape of the Pareto front, and thus, the optimal designs.

7. Metamodel

Metamodeling is a technique used to provide an evaluation of the outputs for complex models at low computational costs. In order to easily estimate the yearly performance indices presented in this article for any set of design parameters without having to launch any simulation, two metamodels (i.e. one for each performance index) will be developed. Among all the metamodeling techniques (e.g. Kriging, Multivariable Adaptive Regression Splines, radial Basis Function [38]), it was chosen to develop the metamodels as second-order polynomial regressions with a few third-order additional terms due to its simplicity. Regarding the third-order coefficients, only the four most important interactions (i.e. third-order interactions between all the WWRs for AGI and between the WWR_S, WWR_W, B_S and B_W for AEL) were added to the metamodels in order to reduce the number of coefficients, thus increasing their the simplicity. Using a metamodel has the effect of introducing errors in the estimation of the model outputs. In addition to the form of the fitting equations, the sampling can also affect the precision of the metamodel. For this article, all 1900 simulation values were used in order to develop the metamodel. An additional 100 simulations were used to test the metamodels with points that were not used to build it.

7.1 Description of the fitting method

It is worth to note that the linear regressions previously presented could be seen as metamodels, but since the summation of the SRCs was relatively low (in particular for AEL) due to non-linear effects, a higher order regression was built. The form of the fitting that was chosen is:

$$Y_n^* = c_0 + \sum_{i=1}^{15} c_i x_i + \sum_{i=1}^{15} \sum_{j\geq i}^{15} c_{ij} x_i x_j + \sum_{i=1}^{4} \sum_{j\geq i}^{4} \sum_{k\geq j}^{4} c_{ijk} x_i x_j x_k \qquad (14)$$

where n refers to either AGI and AEL.

In order to evaluate the regression coefficients (i.e. the c_i, c_{ij} and c_{ijk} from Eq. (14)), the sum of the squared errors between the estimated outputs and the real values from the simulations was minimized. Once the regression coefficients were found, Eq. (14) could be used to evaluate the outputs for any new set of design parameters included in the range of possible values presented in Table 2, as will be evaluated later. Mean errors between the estimated and calculated performance indices have been evaluated as a first validation of the metamodels and have values of 10.28% and 16.12% for AGI and AEL respectively, with coefficient of determination (R^2) of 0.951 and 0.798.

7.2 Validation of metamodels

To assess the capability of the metamodels to correctly determine AEL and AGI for different building designs, a new dataset was generated. A total of 100 new sets of design variables were created using the methodology presented in Section 2. The randomly generated values of the inputs were used in Daysim to produce 100 new simulation results. Then, the evaluation of AEL and AGI from the simulations was compared to that provided by the metamodels for the exact same set of variables. Results are shown in Fig. 11.

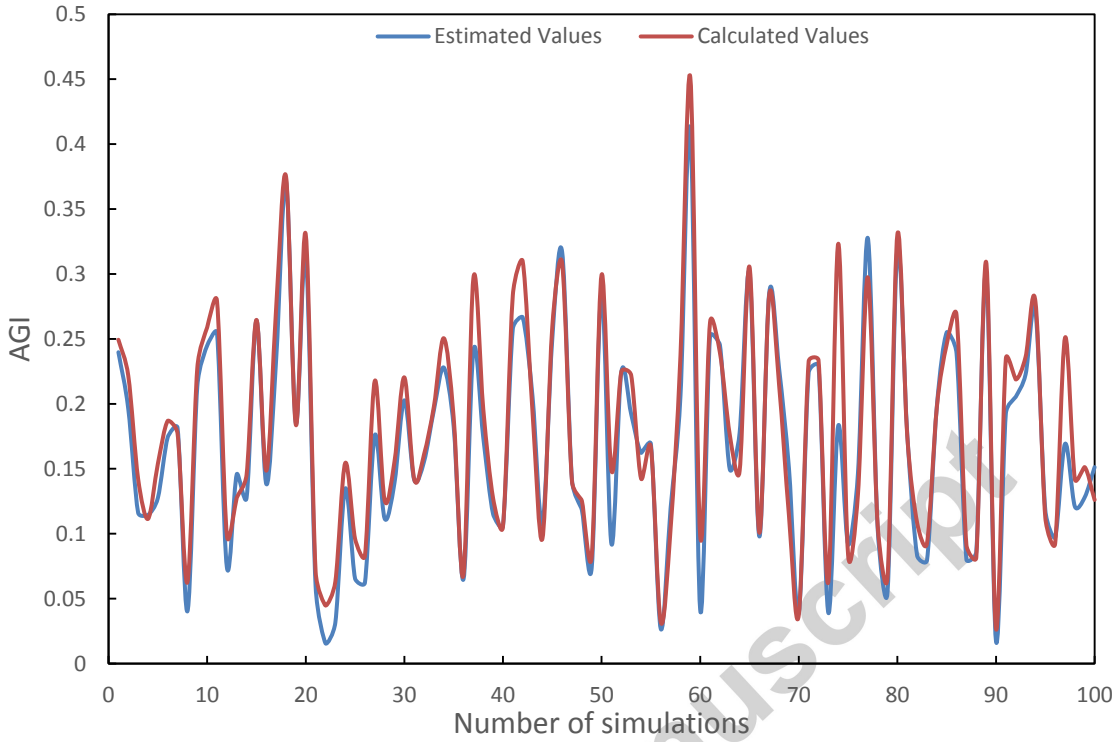

(a)

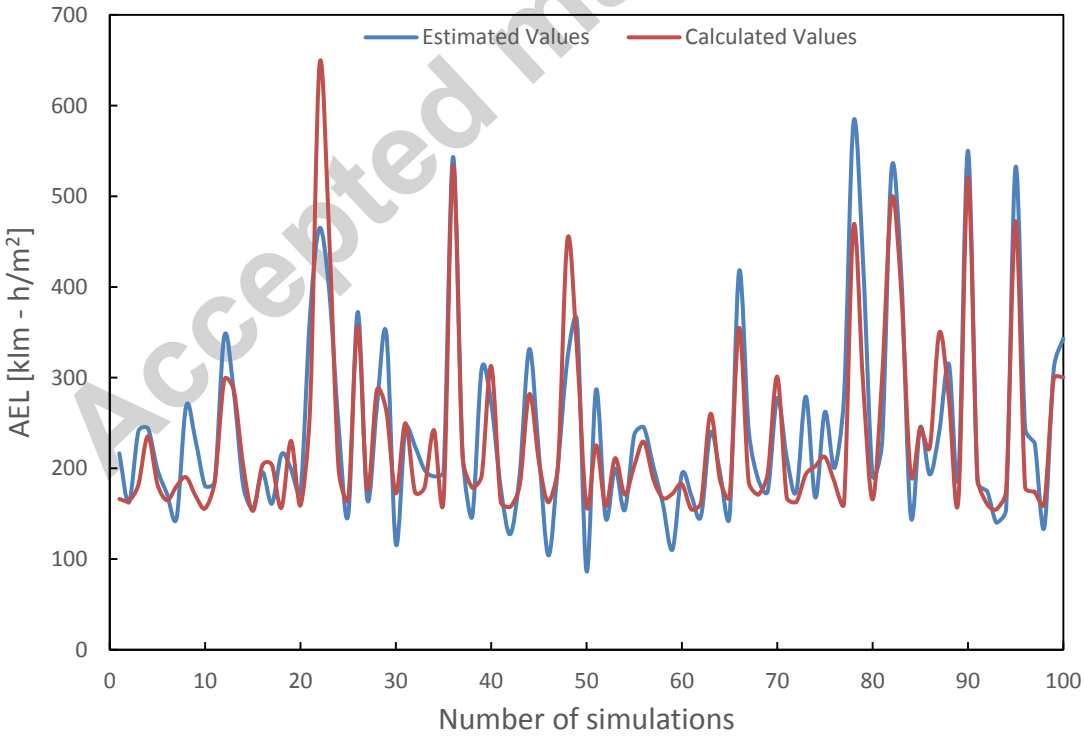

(b)

Figure 11. Comparison between AEL and AGI evaluated from simulations and from the metamodels for 100 additional building designs.

It can be concluded that the metamodels can give a fairly good estimate of the performance indices. The mean errors between the estimated and calculated values were approximately 12.2 and 16.8% with coefficients of determination (R^2) of 0.928 and 0.770, for AGI and AEL respectively. These results are very close to the mean errors and coefficients of determination initially obtained from the calculation of the regression coefficients, which means that the metamodels have the ability to extrapolate efficiently performance index values for different sets of design parameters. The values of the regression coefficients are presented in Annexes A and B. It should be noted that, in the metamodels, the design parameters values have been normalized (see Eq. (4)) and standardized.

Note that other types of correlation than Eq. (14) have also been tested. In particular, linear and quadratic fittings have been considered. In the linear fittings, the coefficients c_{ij} and c_{ijk} of Eq. (14) were set to zero and the coefficients ci were chosen to minimize the error between the correlation and the results. A similar procedure was also used for the quadratic fitting. The coefficients of determination as well as the mean errors are presented in Table 5 as a function of the order of the regressions.

Table 5. Coefficients of determination and mean errors for different orders of regressions.

	AGI		**AEL**	
Order	**Coefficient of determination**	**Mean error [%]**	**Coefficient of determination**	**Mean error [%]**
1	0.790	20.7	0.524	26.2
2	0.928	12.5	0.718	16.8
3	0.928	12.2	0.770	16.8

From these values, one could note an important increase in the accuracy of the metamodels from the first-order to the second-order regression. Adding the third-order interactions had a small impact on AGI evaluation, but significantly increased the

coefficient of determination for AEL. Again, it should be noted that only 20 third-order interactions were considered out of 680 possibilities. The 20 additional terms represent the interactions between four design parameters that were identified as the most significant and considering Fig. 11 and Table 5, it was judged that the metamodels were able to capture the main behavior of AEL and AGI as functions of the design variables. Further improvement of the metamodel would require enlarging the data sample and adding more terms to the fitting.

8. Conclusions

The sensitivity analysis presented in this paper explained which of the selected building design parameters had significant impact on the natural daylighting performance. In order to do so, a building model was developed with the software Daysim and two yearly performance indices (i.e. one concerning glaring and another about the energy annually consumed for lighting) were defined to characterize building designs. Values were randomly attributed to 15 design parameters from a range of possible values for each of them. Then, coefficients of variation and scatterplots have been studied to see graphically if the chosen design parameters had an impact on the outputs of the model. Furthermore, two techniques were used to quantitatively evaluate the impact of the design parameters on the performance indices. Standardized regression coefficients, whose value represents the change in the standard deviation of an output for a change of one standard deviation in a given input, were calculated using a linear regression. Since one of the performance indices was found to have a highly non-linear behavior, a variance-based method was used to more accurately estimate the importance of each design parameter. This last method allowed the calculation of first-order sensitivity indices, as well as the calculation of second-order interactions between the inputs, thus explaining a more important fraction of the variance of the outputs. Using these methods, it was found that every window-to-wall ratio as well as the depth of overhang on the south façade were the parameters that had the most impact on the annual glaring index. Also, the most important interactions for that index were found between all the WWRs and the building aspect ratio. Regarding the annual energy for lighting, the window-to-wall ratios on the west and south façades, two parameters who were discovered to have great interactions,

and the window position on the same façades were found to be the most significant parameters. It should be remembered that these conclusions are valid for the building that was considered. Other locations or occupancy could potentially result in different conclusions. Finally, metamodels were suggested to easily estimate the yearly performance indices for any set of design parameters. Even if the mean errors were found to be important, these metamodels can still be used as a first approximation of the natural daylighting performance indices of a building design.

This article provides building designers with a tool to estimate easily and quickly the daylighting performance of a building using metamodels. The paper explains the methodology that was developed to create these metamodels and which can be used for any set of parameters and locations. Considering the initial computational cost for generating the required dataset from with the sensitivity analysis and metamodels were done, future work could include more design variables, such as the internal wall reflectance, the building typology (e.g., L or H shape buildings) and different window sizes and positions. Other cities and occupancy schedules could also be considered to take into account the effect of being in different climatic contexts. It would also be interesting to include in the model the dynamic control of daylighting by occupants or automated systems [5], [39]. In addition, the results of this work could be coupled with energy performance multivariable analysis in order to optimize building designs from a natural lighting and a building energy consumption view simultaneously. For example, the total energy consumption of the building, including lighting and other end-uses, could be minimized. The models and results of this paper could serve as a one of the building blocks in a broader energy and comfort optimization process.

Acknowledgements

This work was supported by the Natural Sciences and Engineering Research Council of Canada (NSERC). The first author's work is also supported by the Fonds de recherche du Québec – Nature et Technologies (FRQNT).

References

[1] U.S. Energy Information Administration, "How much electricity is used for lighting in the United States?," 06-Sep-2016. [Online]. Available: https://www.eia.gov/tools/faqs/faq.cfm?id=99&t=3. [Accessed: 16-Jan-2017].
[2] Natural Resources Canada, "Lighting," 10-Jan-2017. [Online]. Available: http://www.nrcan.gc.ca/energy/products/categories/lighting/13730. [Accessed: 16-Jan-2017].
[3] J. R. Brodrick, E. D. Petrow, and M. J. Scholand, "Lighting energy consumption trends and R&D opportunities," presented at the Solid State Lighting II, Seattle, Washington, 2002, vol. 4776, pp. 9–17.
[4] C. Kurian, R. Aithal, J. Bhat, and V. George, "Robust control and optimisation of energy consumption in daylight—artificial light integrated schemes," *Light. Res. Technol.*, vol. 40, no. 1, pp. 7–24, Mar. 2008.
[5] A. Tzempelikos and A. K. Athienitis, "The impact of shading design and control on building cooling and lighting demand," *Sol. Energy*, vol. 81, no. 3, pp. 369–382, Mar. 2007.
[6] M.-C. Dubois and Å. Blomsterberg, "Energy saving potential and strategies for electric lighting in future North European, low energy office buildings: A literature review," *Energy Build.*, vol. 43, no. 10, pp. 2572–2582, Oct. 2011.
[7] G. Y. Yun, H. Kim, and J. T. Kim, "Effects of occupancy and lighting use patterns on lighting energy consumption," *Energy Build.*, vol. 46, pp. 152–158, Mar. 2012.
[8] A. D. Galasiu and J. A. Veitch, "Occupant preferences and satisfaction with the luminous environment and control systems in daylit offices: a literature review," *Energy Build.*, vol. 38, no. 7, pp. 728–742, Jul. 2006.
[9] D. Bourgeois, C. Reinhart, and I. Macdonald, "Adding advanced behavioural models in whole building energy simulation: A study on the total energy impact of manual and automated lighting control," *Energy Build.*, vol. 38, no. 7, pp. 814–823, Jul. 2006.
[10] T. Gibson and M. Krarti, "Comparative Analysis of Prediction Accuracy from Daylighting Simulation Tools," *LEUKOS*, vol. 11, no. 2, pp. 49–60, Apr. 2015.
[11] C. Reinhart and A. Fitz, "Findings from a survey on the current use of daylight simulations in building design," *Energy Build.*, vol. 38, no. 7, pp. 824–835, Jul. 2006.
[12] K. S. Lee, K. J. Han, and J. W. Lee, "Feasibility Study on Parametric Optimization of Daylighting in Building Shading Design," *Sustainability*, vol. 8, no. 12, p. 1220, Nov. 2016.
[13] A. Galatioto and M. Beccali, "Aspects and issues of daylighting assessment: A review study," *Renew. Sustain. Energy Rev.*, vol. 66, pp. 852–860, Dec. 2016.
[14] M. Khoroshiltseva, D. Slanzi, and I. Poli, "A Pareto-based multi-objective optimization algorithm to design energy-efficient shading devices," *Appl. Energy*, vol. 184, pp. 1400–1410, Dec. 2016.
[15] International Glazing Database, "Optical data for over 3800 glazing products," 2011. [Online]. Available: https://windows.lbl.gov/materials/igdb/. [Accessed: 01-Jul-2016].
[16] Christoph F. Reinhart, "DAYSIM: Advanced daylight simultaion software," 2016. [Online]. Available: http://daysim.ning.com/. [Accessed: 01-Jun-2016].

[17] J. Mardaljevic, L. Heschong, and E. Lee, "Daylight metrics and energy savings," *Light. Res. Technol.*, vol. 41, no. 3, pp. 261–283, Sep. 2009.
[18] C. F. Reinhart, J. Mardaljevic, and Z. Rogers, "Dynamic Daylight Performance Metrics for Sustainable Building Design," *LEUKOS*, vol. 3, no. 1, pp. 7–31, Jul. 2006.
[19] J. Y. Suk, M. Schiler, and K. Kensek, "Absolute glare factor and relative glare factor based metric: Predicting and quantifying levels of daylight glare in office space," *Energy Build.*, vol. 130, pp. 8–19, Oct. 2016.
[20] A. Pino, W. Bustamante, R. Escobar, and F. E. Pino, "Thermal and lighting behavior of office buildings in Santiago of Chile," *Energy Build.*, vol. 47, pp. 441–449, Apr. 2012.
[21] U. S. D. of Energy, "Energy efficiency of LEDs." Energy Efficiency & Renewable Energy, Mar-2013.
[22] B. Urban and L. Glicksman, "THE MIT DESIGN ADVISOR – A FAST, SIMPLE TOOL FOR ENERGY EFFICIENT BUILDING DESIGN," *IBPSA-USA J.*, vol. 2, no. 1, 2006.
[23] M. A. Lehar, "A simulation tool for the estimation and optimization of electrical lighting energy," Massachusetts Institute of Technology, 2003.
[24] S. Carlucci, G. Cattarin, F. Causone, and L. Pagliano, "Multi-objective optimization of a nearly zero-energy building based on thermal and visual discomfort minimization using a non-dominated sorting genetic algorithm (NSGA-II)," *Energy Build.*, vol. 104, pp. 378–394, Oct. 2015.
[25] "Uniformly distributed random numbers - MATLAB rand." [Online]. Available: https://www.mathworks.com/help/matlab/ref/rand.html. [Accessed: 12-Jul-2017].
[26] A. Saltelli *et al.*, *Global Sensitivity Analysis. The Primer*. John Wiley & Sons, Ltd, 2007.
[27] R. Singh, I. J. Lazarus, and V. V. N. Kishore, "Uncertainty and sensitivity analyses of energy and visual performances of office building with external venetian blind shading in hot-dry climate," *Appl. Energy*, vol. 184, pp. 155–170, Dec. 2016.
[28] Z. Long, H. Li, X. Bu, W. Ma, and L. Zhao, "Solar radiation on vertical surfaces for building application in different climate zones across China," *J. Renew. Sustain. Energy*, vol. 5, no. 2, pp. 1–7, Mar. 2013.
[29] V. Granadeiro, J. P. Duarte, J. R. Correia, and V. M. S. Leal, "Building envelope shape design in early stages of the design process: Integrating architectural design systems and energy simulation," *Autom. Constr.*, vol. 32, pp. 196–209, Jul. 2013.
[30] R. P. Leslie, "Capturing the daylight dividend in buildings: why and how?," *Build. Environ.*, vol. 38, no. 2, pp. 381–385, Feb. 2003.
[31] J. Nossent, P. Elsen, and W. Bauwens, "Sobol' sensitivity analysis of a complex environmental model," *Environ. Model. Softw.*, vol. 26, no. 12, pp. 1515–1525, Dec. 2011.
[32] E. Plischke, "An effective algorithm for computing global sensitivity indices (EASI)," *Reliab. Eng. Syst. Saf.*, vol. 95, no. 4, pp. 354–360, Apr. 2010.
[33] C. E. Ochoa, M. B. C. Aries, E. J. van Loenen, and J. L. M. Hensen, "Considerations on design optimization criteria for windows providing low energy consumption and high visual comfort," *Appl. Energy*, vol. 95, pp. 238–245, Jul. 2012.

[34] E. Ghisi and J. A. Tinker, "An Ideal Window Area concept for energy efficient integration of daylight and artificial light in buildings," *Build. Environ.*, vol. 40, no. 1, pp. 51–61, Jan. 2005.
[35] W. J. Fisk, "Health and productivity gains from better indoor environments and their relationship with building energy efficiency," *Annu. Rev. Energy Environ.*, vol. 25, no. 1, pp. 537–566, 2000.
[36] Silvia Cammarano, Anna Pellegrino, Valerio R.M. Lo Verso, and Chiara Aghemo, "Daylighting Design for Energy Saving in a Building Global Energy Simulation Context," *Energy Procedia*, vol. 78, pp. 364–369, 2015.
[37] M. Krarti, P. M. Erickson, and T. C. Hillman, "A simplified method to estimate energy savings of artificial lighting use from daylighting," *Build. Environ.*, vol. 40, no. 6, pp. 747–754, Jun. 2005.
[38] Y. F. Li, S. H. Ng, M. Xie, and T. N. Goh, "A systematic comparison of metamodeling techniques for simulation optimization in Decision Support Systems," *Appl. Soft Comput.*, vol. 10, no. 4, pp. 1257–1273, Sep. 2010.
[39] R. Baetens, B. P. Jelle, and A. Gustavsen, "Properties, requirements and possibilities of smart windows for dynamic daylight and solar energy control in buildings: A state-of-the-art review," *Sol. Energy Mater. Sol. Cells*, vol. 94, no. 2, pp. 87–105, Feb. 2010.

Figure captions

Figure 1 Schematic representation of the building design.

Figure 2 Mesh independence study for the daylight simulations: (a) AGI and (b) AEL as a function of the number of cells for two cases.

Figure 3 Scatterplots of (a) AGI and (b) AEL as functions of the window-to-wall ratio of the south façade.

Figure 4 Coefficients of variation for AGI and AEL as functions of the number of simulations.

Figure 5 Standardized regression coefficients as functions of the number of simulations for: (a) AGI and (b) AEL.

Figure 6 Standardized regression coefficients for every design parameter and both performance indices (AEL and AGI).

Figure 7 Summation of the first-order sensitivity indices as a function of the number of simulations.

Figure 8 First-order sensitivity indices and square of standardized regression coefficients as functions of the design variables for: (a) AGI and (b) AEL.

Annex A: Regression coefficients for the evaluation of AGI with Eq. (14)

y-intercept	0.1687	x_1x_{11}	-0.0176	x_3x_{10}	0.0058	x_5x_{13}	0.0013	x_8x_{12}	-0.0002	$x_{13}x_{13}$	-0.0050
W/L (x_1)	-0.0687	x_1x_{12}	0.0006	x_3x_{11}	0.0013	x_5x_{14}	0.0015	x_8x_{13}	0.0039	$x_{13}x_{14}$	0.0003
WWR_N (x_2)	-0.0951	x_1x_{13}	-0.0041	x_3x_{12}	0.0007	x_5x_{15}	0.0023	x_8x_{14}	0.0054	$x_{13}x_{15}$	0.0041
WWR_W (x_3)	-0.0100	x_1x_{14}	0.0061	x_3x_{13}	0.0053	x_6x_6	0.0099	x_8x_{15}	0.0037	$x_{14}x_{14}$	-0.0166
WWR_S (x_4)	-0.0655	x_1x_{15}	-0.0002	x_3x_{14}	0.0010	x_6x_7	-0.0043	x_9x_9	0.0012	$x_{14}x_{15}$	0.0008
WWR_E (x_5)	-0.0158	x_2x_2	0.0532	x_3x_{15}	0.0018	x_6x_8	0.0028	x_9x_{10}	-0.0020	$x_{15}x_{15}$	-0.0071
VT_N (x_6)	-0.0172	x_2x_3	0.0207	x_4x_4	0.0659	x_6x_9	-0.0034	x_9x_{11}	0.0022	$x_2x_2x_2$	-0.0177
VT_W (x_7)	0.0000	x_2x_4	0.0049	x_4x_5	0.0135	x_6x_{10}	-0.0005	x_9x_{12}	0.0038	$x_2x_2x_3$	-0.0084
VT_S (x_8)	-0.0027	x_2x_5	0.0144	x_4x_6	0.0034	x_6x_{11}	-0.0025	x_9x_{13}	-0.0005	$x_2x_2x_4$	0.0011
VT_E (x_9)	0.0101	x_2x_6	0.0546	x_4x_7	0.0008	x_6x_{12}	0.0034	x_9x_{14}	0.0018	$x_2x_2x_5$	-0.0036
θ (x_{10})	-0.0007	x_2x_7	0.0047	x_4x_8	0.0578	x_6x_{13}	-0.0053	x_9x_{15}	0.0044	$x_2x_3x_3$	-0.0063
D (x_{11})	0.0320	x_2x_8	0.0031	x_4x_9	-0.0026	x_6x_{14}	-0.0032	$x_{10}x_{10}$	0.0028	$x_2x_3x_4$	0.0010
B_N (x_{12})	-0.0028	x_2x_9	-0.0016	x_4x_{10}	-0.0003	x_6x_{15}	0.0050	$x_{10}x_{11}$	0.0003	$x_2x_3x_5$	-0.0021
B_W (x_{13})	-0.0016	x_2x_{10}	0.0022	x_4x_{11}	-0.0312	x_7x_7	0.0036	$x_{10}x_{12}$	0.0014	$x_2x_4x_4$	-0.0020
B_S (x_{14})	0.0049	x_2x_{11}	-0.0043	x_4x_{12}	0.0009	x_7x_8	-0.0027	$x_{10}x_{13}$	0.0020	$x_2x_4x_5$	0.0013
B_E (x_{15})	-0.0102	x_2x_{12}	0.0044	x_4x_{13}	0.0005	x_7x_9	0.0021	$x_{10}x_{14}$	0.0008	$x_2x_5x_5$	-0.0062
x_1x_1	0.0496	x_2x_{13}	0.0004	x_4x_{14}	0.0074	x_7x_{10}	0.0040	$x_{10}x_{15}$	-0.0030	$x_3x_3x_3$	-0.0067
x_1x_2	0.0283	x_2x_{14}	0.0018	x_4x_{15}	0.0014	x_7x_{11}	-0.0024	$x_{11}x_{11}$	0.0033	$x_3x_3x_4$	-0.0043
x_1x_3	-0.0280	x_2x_{15}	0.0012	x_5x_5	0.0317	x_7x_{12}	0.0013	$x_{11}x_{12}$	0.0001	$x_3x_3x_5$	-0.0020
x_1x_4	0.0382	x_3x_3	0.0163	x_5x_6	-0.0023	x_7x_{13}	0.0068	$x_{11}x_{13}$	-0.0007	$x_3x_4x_4$	-0.0117
x_1x_5	-0.0237	x_3x_4	0.0219	x_5x_7	0.0002	x_7x_{14}	0.0038	$x_{11}x_{14}$	-0.0053	$x_3x_4x_5$	-0.0036
x_1x_6	0.0297	x_3x_5	0.0095	x_5x_8	0.0083	x_7x_{15}	-0.0007	$x_{11}x_{15}$	-0.0014	$x_3x_5x_5$	-0.0020
x_1x_7	-0.0169	x_3x_6	0.0001	x_5x_9	0.0263	x_8x_8	-0.0058	$x_{12}x_{12}$	-0.0099	$x_4x_4x_4$	-0.0315
x_1x_8	0.0284	x_3x_7	0.0312	x_5x_{10}	-0.0073	x_8x_9	-0.0082	$x_{12}x_{13}$	0.0006	$x_4x_4x_5$	-0.0056
x_1x_9	-0.0155	x_3x_8	0.0058	x_5x_{11}	0.0004	x_8x_{10}	-0.0038	$x_{12}x_{14}$	0.0003	$x_4x_5x_5$	-0.0046
x_1x_{10}	0.0025	x_3x_9	-0.0083	x_5x_{12}	-0.0009	x_8x_{11}	-0.0151	$x_{12}x_{15}$	0.0011	$x_5x_5x_5$	-0.0178

Annex B: Regression coefficients for the evaluation of AEL with Eq. (14)

y-intercept	241.36	x_1x_{11}	-2.15	x_3x_{10}	-0.64	x_5x_{13}	-2.43	x_8x_{12}	-12.02	$x_{13}x_{13}$	195.64
W/L (x_1)	24.28	x_1x_{12}	-1.76	x_3x_{11}	-28.02	x_5x_{14}	-7.97	x_8x_{13}	-6.75	$x_{13}x_{14}$	-37.13
WWR_N (x_2)	-56.45	x_1x_{13}	-3.53	x_3x_{12}	9.34	x_5x_{15}	3.71	x_8x_{14}	-1.75	$x_{13}x_{15}$	-1.10
WWR_W (x_3)	-577.97	x_1x_{14}	-4.00	x_3x_{13}	-6.45	x_6x_6	49.62	x_8x_{15}	-14.89	$x_{14}x_{14}$	227.37
WWR_S (x_4)	-467.11	x_1x_{15}	-2.05	x_3x_{14}	-77.97	x_6x_7	-1.97	x_9x_9	7.63	$x_{14}x_{15}$	-8.25
WWR_E (x_5)	-69.64	x_2x_2	8.93	x_3x_{15}	-2.64	x_6x_8	9.24	x_9x_{10}	5.72	$x_{15}x_{15}$	6.10
VT_N (x_6)	-43.23	x_2x_3	38.87	x_4x_4	317.08	x_6x_9	-24.83	x_9x_{11}	-6.11	$x_3x_3x_3$	-138.36
VT_W (x_7)	-41.02	x_2x_4	37.02	x_4x_5	12.10	x_6x_{10}	7.80	x_9x_{12}	-7.53	$x_3x_3x_4$	-195.31
VT_S (x_8)	-58.26	x_2x_5	4.12	x_4x_6	45.23	x_6x_{11}	-16.67	x_9x_{13}	0.97	$x_3x_3x_{13}$	-63.22
VT_E (x_9)	-12.83	x_2x_6	-6.12	x_4x_7	53.82	x_6x_{12}	-8.38	x_9x_{14}	-8.58	$x_3x_3x_{14}$	34.73
θ (x_{10})	-21.23	x_2x_7	14.23	x_4x_8	10.55	x_6x_{13}	-19.92	x_9x_{15}	-13.90	$x_3x_4x_4$	-163.10
D (x_{11})	93.46	x_2x_8	9.35	x_4x_9	17.27	x_6x_{14}	-8.49	$x_{10}x_{10}$	-0.74	$x_3x_4x_{13}$	53.69
B_N (x_{12})	20.40	x_2x_9	11.40	x_4x_{10}	8.28	x_6x_{15}	-11.15	$x_{10}x_{11}$	2.17	$x_3x_4x_{14}$	19.11
B_W (x_{13})	76.58	x_2x_{10}	5.10	x_4x_{11}	-8.93	x_7x_7	13.78	$x_{10}x_{12}$	1.02	$x_3x_{13}x_{13}$	17.17
B_S (x_{14})	35.96	x_2x_{11}	-18.92	x_4x_{12}	2.72	x_7x_8	23.28	$x_{10}x_{13}$	3.08	$x_3x_{13}x_{14}$	-0.59
B_E (x_{15})	45.76	x_2x_{12}	-3.07	x_4x_{13}	-153.07	x_7x_9	5.52	$x_{10}x_{14}$	-2.82	$x_3x_{14}x_{14}$	-7.02
x_1x_1	-3.91	x_2x_{13}	-19.87	x_4x_{14}	5.84	x_7x_{10}	-19.28	$x_{10}x_{15}$	2.00	$x_4x_4x_4$	-95.34
x_1x_2	-17.26	x_2x_{14}	-15.15	x_4x_{15}	0.04	x_7x_{11}	-12.71	$x_{11}x_{11}$	8.09	$x_4x_4x_{13}$	69.08
x_1x_3	19.09	x_2x_{15}	-0.78	x_5x_5	10.72	x_7x_{12}	-12.41	$x_{11}x_{12}$	0.52	$x_4x_4x_{14}$	-41.36
x_1x_4	3.00	x_3x_3	474.09	x_5x_6	8.47	x_7x_{13}	-19.22	$x_{11}x_{13}$	8.00	$x_4x_{13}x_{13}$	-5.22
x_1x_5	14.39	x_3x_4	460.42	x_5x_7	0.75	x_7x_{14}	-23.64	$x_{11}x_{14}$	3.39	$x_4x_{13}x_{14}$	-4.67
x_1x_6	-20.77	x_3x_5	17.78	x_5x_8	20.29	x_7x_{15}	-3.89	$x_{11}x_{15}$	-1.30	$x_4x_{14}x_{14}$	15.43
x_1x_7	0.11	x_3x_6	38.40	x_5x_9	0.11	x_8x_8	5.56	$x_{12}x_{12}$	8.44	$x_{13}x_{13}x_{13}$	-131.13
x_1x_8	-7.73	x_3x_7	-1.60	x_5x_{10}	-2.10	x_8x_9	14.67	$x_{12}x_{13}$	5.74	$x_{13}x_{13}x_{14}$	18.47
x_1x_9	-1.30	x_3x_8	56.19	x_5x_{11}	-7.98	x_8x_{10}	16.03	$x_{12}x_{14}$	-1.16	$x_{13}x_{14}x_{14}$	28.25
x_1x_{10}	-5.43	x_3x_9	23.76	x_5x_{12}	0.18	x_8x_{11}	-18.36	$x_{12}x_{15}$	0.33	$x_{14}x_{14}x_{14}$	-156.11

Highlights

- Lighting in buildings demand significant energy and influences comfort
- The impact of 15 design variables on daylight performance was assessed
- Glare and energy consumption of artificial lighting were considered
- Window-to-wall ratios and overhang were among the most influential parameters
- Metamodels were developed to determine quickly daylight performance